DEPARTMENT OF ELECTRICAL ENGINEERING
COOLEY ELECTRONICS LABORATORY

Quarterly Progress Report No. 6

Study and Investigation of a UHF-VHF Antenna

Period Covering July 1, 1961 to October 1, 1961

Prepared by: J. C. PALAIS
            A. I. SIMANYI
            R. M. KALAFUS
            A. T. ADAMS
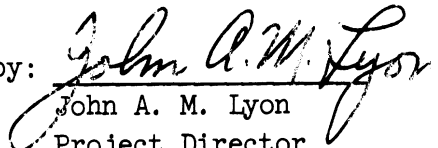
Approved by: J. A. M. LYON

THE UNIVERSITY OF MICHIGAN

COLLEGE OF ENGINEERING
Department of Electrical Engineering
Colley Electronics Laboratory

Quarterly Progress Report No. 6
Period Covering July 1, 1961 to October 1, 1961

STUDY AND INVESTIGATION OF A UHF-VHF ANTENNA

A. T. Adams
R. M. Kalafus
J. C. Palais
A. I. Simanyi

Approved by: *John A. M. Lyon*
John A. M. Lyon
Project Director

ORA Project 03667

under contract with:

administered through:

OFFICE OF RESEARCH ADMINISTRATION   ANN ARBOR

November 1961

TABLE OF CONTENTS

LIST OF FIGURES

iv

ABSTRACT

Several theoretical and experimental problems were studied during this period. The study of diffraction of a plane wave by a ferrite sphere was extended to include a small lossy inner sphere enclosed within and concentric with the original ferrite sphere. Computer results show that the total power absorbed by the inner sphere rises to peak values of about 500 times the power incident upon a cross-section area equal to that of the large ferrite sphere. A summary of the mathematical results has been compiled for the theoretical study of the diffraction of an incident plane wave by a long ferrite cylinder. The total power passing through the cylinder has been evaluated on the computer and compared with the power incident upon a cross-section area equal to that of the cylinder in free space. The ratio rises to peaks greater than ten.

A study of the scattering of a plane wave by a ferrite spheroid was initiated, but, because of the need for more experimental activity in other areas, temporarily discontinued. The basic analytical steps are outlined. The radiation from a material-filled rectangular waveguide H plane sectoral horn has been analyzed. Computer results will be given in the next quarterly report.

The problem of the radiation from a ferrite-filled double taper horn fed by a rectangular waveguide has been analyzed mathematically.

1. REPORTS, TRAVEL, AND VISITORS

During this period no reports were issued and no one visited the project. A trip was made to Wright-Patterson Air Force Base on September 5 to discuss project matters. CEL personnel present were CEL Director B.F. Barton, Professor John A.M. Lyon, A.T. Adams, R.M. Kalafus, and J.C. Palais. A number of VHF and microwave antenna problems of interest to the Aeronautical Systems Division were discussed in connection with possible extensions of the contract.

2. FACTUAL DATA

2.1 PLANE WAVE INCIDENT ON A MATERIAL SPHERE IN WHICH IS IMBEDDED A LOSSY INNER-SPHERE

2.1.1 <u>General Discussion</u>.—The sphere problem has been further modified to include an inner material sphere of complex μ and ϵ. There are two reasons for solving this problem. First, the integration of the Poynting vector over the inner sphere will yield the power absorbed by it. This can be compared to the amount of power incident upon an area in free space equal to the cross-section area of the large sphere, or to the power absorbed by the same inner sphere in free space. The second reason is the following: in an actual antenna the energy is carried away from the antenna into the receiver through the feed; the waves are not reflected exactly as they would be if the antenna were shorted at the terminals. By postulating a loss over the volume of the

inner, poorly conducting sphere, one can approximate the feed power by a distributed heat loss. This then yields information about the effect of the feed on the field distributions in and around the sphere.

The mathematics of the derivation is given in the section entitled "Mathematical Analysis." The interior field coefficients are given in Figs. 1 and 2 as a function of outer radius with an inner radius of .01 λ_0 = .1 λ_1.

A lossy conductor will have the parameters $\mu = \mu_0$, $\epsilon = \epsilon' - j(\epsilon'' + \frac{\sigma}{\omega})$. If the propagation constant $(k = \omega \sqrt{\mu \epsilon})$ is allowed to be complex, the radial functions must be likewise complex, so that there is a net real part of the power expression greater than zero. The problem was programmed for the IBM-704 computer using the MAD compiler. The expression for the ratio of power absorbed to the power incident (πa^2 x the incident power density) is plotted as a function of normalized radius in Fig. 3. This shows that the power absorbed can be as much as 500 times the power which would pass through the large circular area in free space. Thus the energy must be concentrated toward the sphere near these resonant points.

It is felt that the approach used here may help solve many antenna problems: investigation of the energy distribution of the scattered field can be used to interpret antenna problems and provide some design criteria. The results will be extended and a more complete discussion and interpretation given later.

2.1.2 <u>Mathematical Analysis</u>.—A concentric sphere interior to the original material sphere is postulated, and specified to be of a lossy material. As with an inner lossless metallic sphere, the field solutions in the inter-
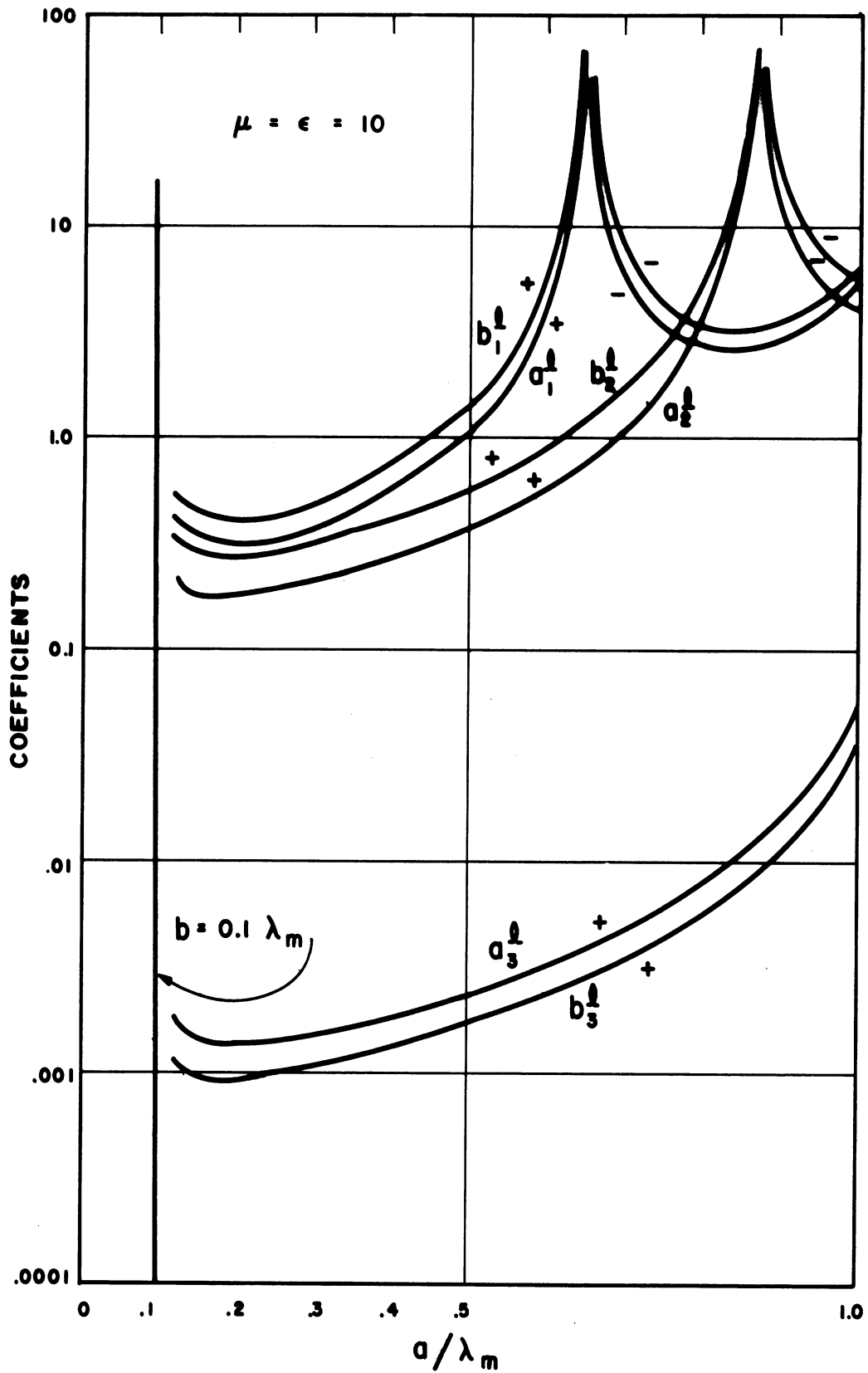
Fig. 1. Field coefficients, real part

3
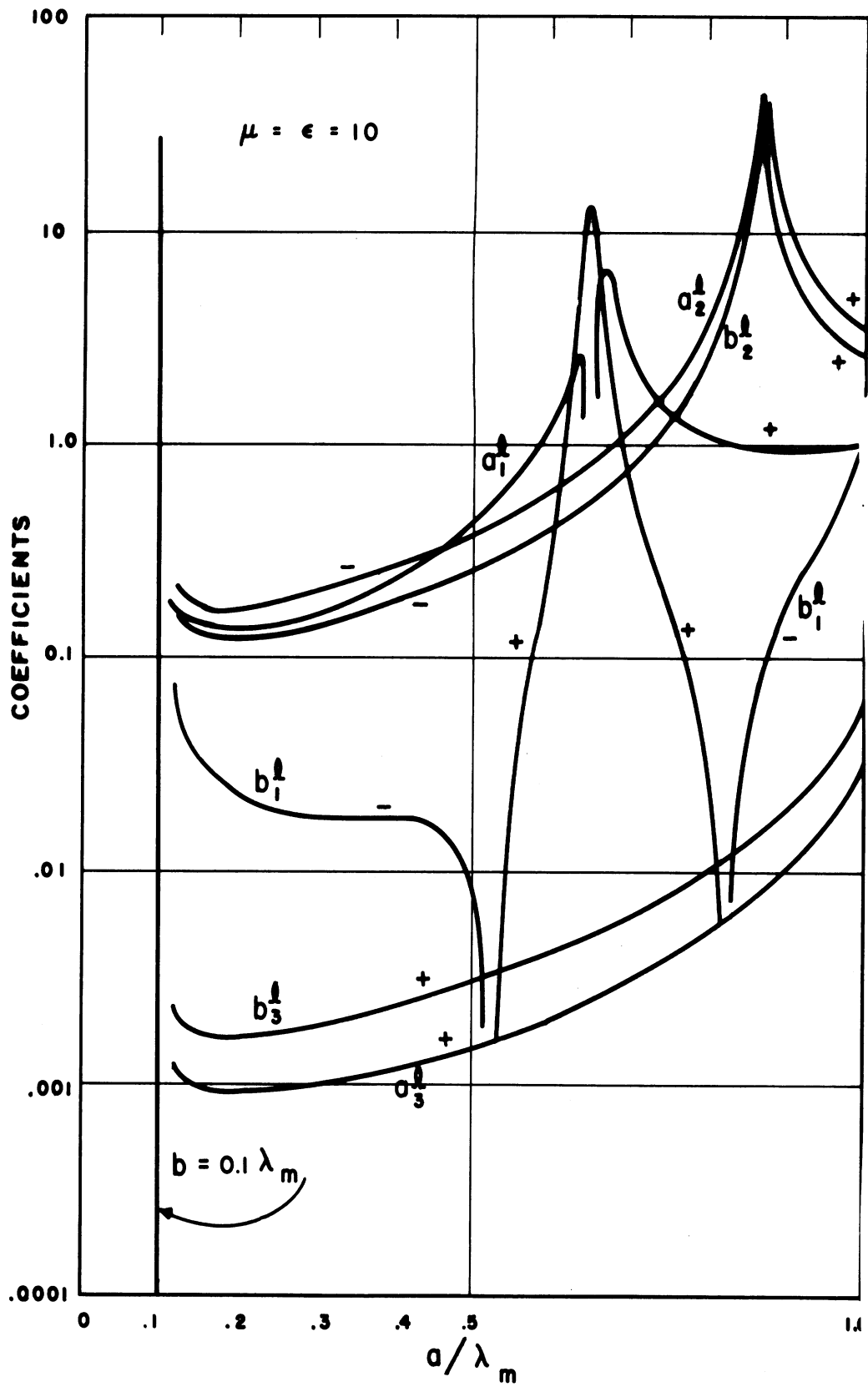
Fig. 2. Field coefficients, imaginary part.

4

Fig. 3. Power absorption ratio.

INNER BOUNDARY AT
$r = b = 0.1\lambda_m$

b^2/a^2

ABSORPTION RATIO =

$$\frac{\text{POWER ABSORBED IN DISSIPATING SPHERE}}{\text{INCIDENT WAVE POWER DENSITY} \times \pi a^2}$$

INNER SPHERE: $\mu = 1$
$\epsilon = -j$
INTERMEDIATE REGION: $\mu = 10$
$\epsilon = 10$

ABSORPTION RATIO

$a/\lambda_m \longrightarrow$

mediate medium must be composed of Bessel and Neumann functions of half order. The inner sphere has only terms involving Bessel functions. This gives rise to eight simultaneous equations, allowing solution of any set of coefficients. The losses in the inner sphere can be treated by allowing μ and ϵ to become complex. One can then integrate the Poynting vector over the sphere to find the power absorbed.

The intermediate medium fields can be expressed by the same set of equations as for an inner conducting sphere.

$$\bar{E}_t = E_0 e^{j\omega t} \sum_{n=1}^{\infty} j^n \frac{2n+1}{n(n+1)} \left[a_n^t \bar{M}_{o1n}^{(1)} + c_n^t \bar{M}_{o1n}^{(2)} - j b_n^t \bar{N}_{e1n}^{(1)} - j d_n^t \bar{N}_{e1n}^{(2)} \right]$$

$$\bar{H}_t = -\sqrt{\frac{\epsilon_1}{\mu_1}}\, E_0 e^{j\omega t} \sum_{n=1}^{\infty} j^n \frac{2n+1}{n(n+1)} \left[b_n^t \bar{M}_{e1n}^{(1)} + d_n^t \bar{M}_{e1n}^{(2)} + j a_n^t \bar{N}_{o1n}^{(1)} + j c_n^t \bar{N}_{o1n}^{(2)} \right] \tag{1}$$

where:

the superscript (2) denotes Bessel functions of the second kind. The interior fields are represented by the coefficients a_n^ℓ and b_n^ℓ.

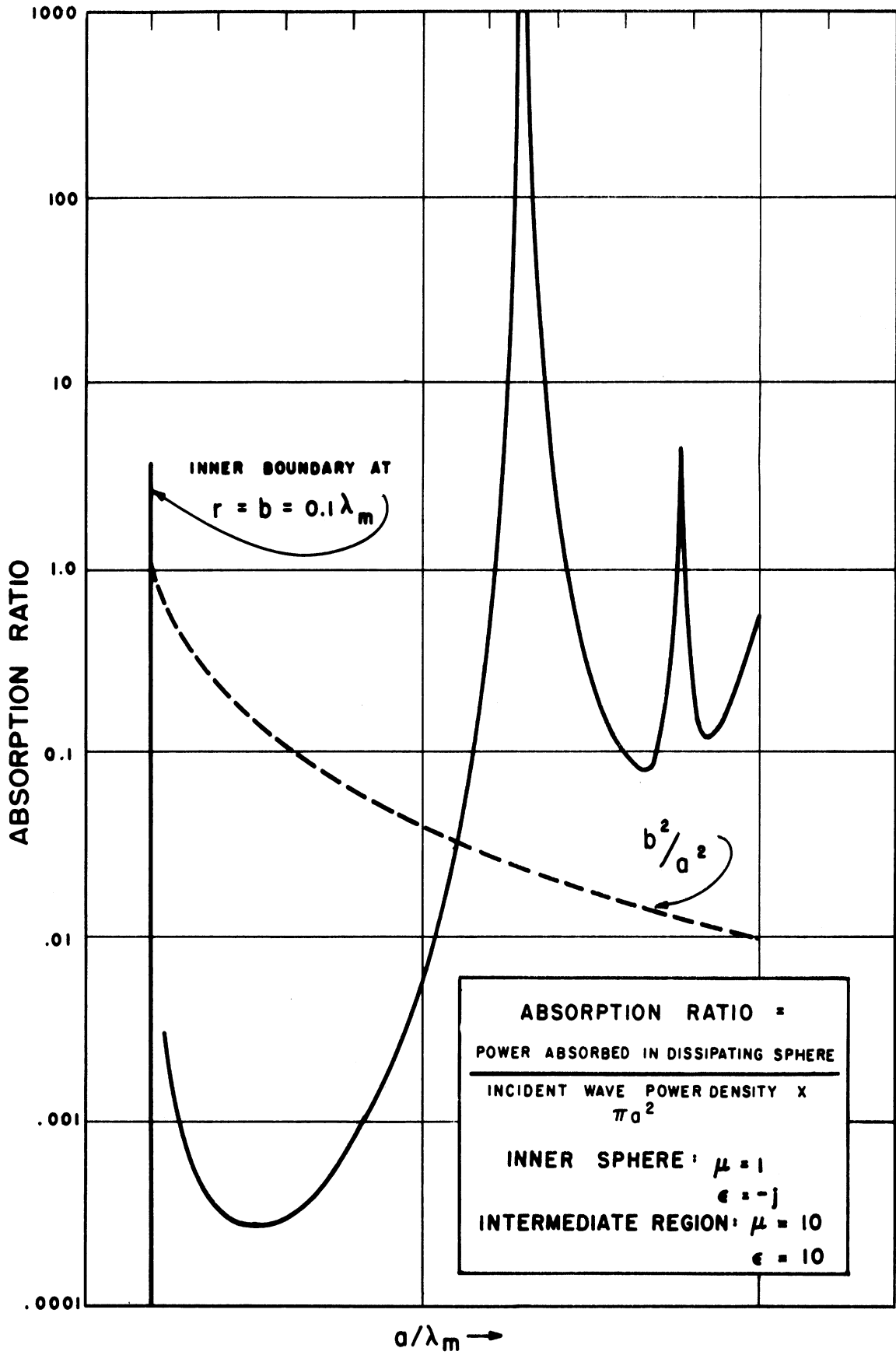$$\bar{E}_\ell = E_0 e^{j\omega t} \sum_{n=1}^{\infty} j^n \frac{2n+1}{n(n+1)} \left[a_n^\ell \bar{M}_{o1n}^{(1)} - j b_n^\ell \bar{N}_{e1n}^{(1)} \right]$$

$$\bar{H}_\ell = -\sqrt{\frac{\epsilon_2}{\mu_2}}\, E_0 e^{j\omega t} \sum_{n=1}^{\infty} j^n \frac{2n+1}{n(n+1)} \left[b_n^\ell \bar{M}_{e1n}^{(1)} + j a_n^\ell \bar{N}_{o1n}^{(1)} \right] \tag{2}$$

where:

ϵ_2 and μ_2 are the complex permittivity and permeability of the inner sphere. There are eight equations resulting from equating the tangential $\bar{E}$ and $\bar{H}$ vectors at $r = a$ and $r = b$.

$$a_n^t S_n(k_1 a) + c_n^t C_n(k_1 a) - K_1 a_n^s R_n^{(2)}(k_o a) = K_1 S_n(k_o a)$$

$$a_n^t S_n'(k_1 a) + c_n^t C_n'(k_1 a) - \mu_1 a_n^s R_n'^{(2)}(k_o a) = \mu_1 S_n'(k_o a)$$

$$K_1 a_n^\ell S_n(k_2 b) = K_2 a_n^t S_n(k_1 b) + K_2 c_n^t C_n(k_1 b)$$

$$\mu_1 a_n^\ell S_n'(k_2 b) = \mu_2 a_n^t S_n'(k_1 b) + \mu_2 c_n^t C_n'(k_1 b) \tag{3}$$

$$b_n^t S_n(k_1 a) + d_n^t C_n(k_1 a) - \mu_1 b_n^s R_n^{(2)}(k_o a) = \mu_1 S_n(k_o a)$$

$$b_n^t S_n'(k_1 a) + d_n^t C_n'(k_1 a) - K_1 b_n^s R_n'^{(2)}(k_o a) = K_1 S_n'(k_o a)$$

$$\mu_1 b_n^\ell S_n(k_2 b) = \mu_2 b_n^t S_n(k_1 b) + \mu_2 d_n^t C_n(k_1 b)$$

$$K_1 b_n^\ell S_n'(k_2 b) = K_2 b_n^t S_n'(k_1 b) + K_2 d_n^t C_n'(k_1 b) \tag{4}$$

Here μ_1, μ_2 are the relative permeabilities and $K_i = k_i/k_o$. The solutions for the six interior coefficients are:

$$a_n^\ell = \frac{j\mu_1\mu_2 K_1 K_2}{\mu_1\mu_2 K_1 \psi_a - \mu_1^2 K_2 \psi_b - \mu_2 K_1^2 \psi_c + \mu_1 K_1 K_2 \psi_d}$$

$$b_n^\ell = \frac{j\mu_1\mu_2 K_1 K_2}{\mu_1 K_1 K_2 \psi_a - \mu_2 K_1^2 \psi_b - \mu_1^2 K_2 \psi_c + \mu_1\mu_2 K_1 \psi_d} \tag{5}$$

$$a_n^t = a_n^\ell \frac{[K_1\mu_2 S_n(k_2 b)C_n'(k_1 b) - K_2\mu_1 S_n'(k_2 b)C_n(k_1 b)]}{\mu_2 K_2}$$

$$b_n^t = b_n^\ell \frac{[\mu_1 K_2 S_n(k_2 b)C_n'(k_1 b) - \mu_2 K_1 S_n'(k_2 b)C_n(k_1 b)]}{\mu_2 K_2}$$

$$c_n^t = a_n^\ell \frac{[K_1\mu_2 S_n(k_2 b)S_n'(k_1 b) - K_2\mu_1 S_n'(k_2 b)S_n(k_1 b)]}{\mu_2 K_2}$$

$$d_n^t = b_n^\ell \frac{[\mu_1 K_2 S_n(k_2 b)S_n'(k_1 b) - \mu_2 K_1 S_n'(k_2 b)S_n(k_1 b)]}{\mu_2 K_2} \tag{6}$$

where:

$$\psi_a = R_n'^{(2)}(k_0 a)S_n(k_2 b)[C_n'(k_1 b)S_n(k_1 a) - S_n'(k_1 b)C_n(k_1 a)]$$

$$\psi_b = R_n'^{(2)}(k_0 a)S_n'(k_2 b)[C_n(k_1 b)S_n(k_1 a) - S_n(k_1 b)C_n(k_1 a)]$$

$$\psi_c = R_n^{(2)}(k_0 a)S_n(k_2 b)[C_n'(k_1 b)S_n'(k_1 a) - S_n'(k_1 b)C_n'(k_1 a)]$$

$$\psi_d = R_n^{(2)}(k_0 a)S_n'(k_2 b)[C_n(k_1 b)S_n'(k_1 a) - S_n(k_1 b)C_n'(k_1 a)] \tag{7}$$

It can be shown from the propagation equation

$$k^2 = \omega^2 \mu\epsilon - j\omega\sigma\mu \tag{8}$$

that losses due to dipole friction in a dielectric (which can be represented by the imaginary part of a complex permittivity) have the same effect on the propagation constant as conductive losses at a given frequency. Thus conductive losses can be simulated by allowing ϵ to become complex; one can then allow the inner sphere to be a lossy conducting surface by letting $\epsilon = \epsilon' - \epsilon''$.

Then $k^2 = \omega \sqrt{\mu_0(\epsilon' - j\epsilon'')}$. One can then integrate over the inner surface and

find the total power absorbed.

This can be calculated by integrating the normal component of the Poynting vector over the surface. Let Γ denote the surface of the sphere. The Poynting vector is defined by $\bar{S} = 1/2 \, \text{Re} \, \{E \times H^*\}$; the surface integration is

$$\iint_\Gamma \bar{S} \cdot \hat{n} \, da = b^2 \int_{\theta=0}^{\pi} \int_{\phi=0}^{2\pi} (\bar{S} \cdot \hat{n}) \sin\theta \, d\theta \, d\phi \qquad (9)$$

where:

$$\bar{S} \cdot \hat{n} = 1/2 \, \text{Re} \, \{\bar{E} \times \bar{H}^*\} \cdot a_r^{\wedge} = -1/2 \, \text{Re} \, \{E_\theta H_\phi^* - E_\phi H_\theta^*\} \qquad (10)$$

where the asterisk denotes the complex conjugate quantity.
Substituting the field equations,

$$\iint \{E_\theta H_\phi^*\} da = j\sqrt{\frac{\epsilon_2}{\mu_2}} \, E_0^2 \pi \sum_{n=1}^{\infty} \sum_{m=1}^{\infty} \frac{2n+1}{n(n+1)} \cdot \frac{2m+1}{m(m+1)} \cdot$$

$$\left\{ + |a_n^t|^2 \frac{S_n(k_2 b)}{k_2 b} \cdot \frac{S_m'(k_2 b)^*}{k_2 b^*} \int_{\theta=0}^{\pi} \frac{P_n^1(\cos\theta) P_m^1(\cos\theta)}{\sin\theta} \, d\theta \qquad (11) \right.$$

$$\left. - |b_n^t|^2 \cdot \frac{S_n'(k_2 b)}{k_2 b} \cdot \frac{S_m(k_2 b)^*}{k_2 b^*} \cdot \int_{\theta=0}^{\pi} \frac{\partial P_n^1(\cos\theta)}{\partial\theta} \frac{\partial P_m^1(\cos\theta)}{\partial\theta} \sin\theta \, d\theta \right\}$$

The terms involving a_n^t and b_n^t have an integration involving $\int_0^{2\pi} \sin\phi \cos\phi \, d\phi \equiv 0$, so that these cross-terms do not contribute.

$$\iint \{E_\phi H_\theta^*\} da = j\sqrt{\frac{\epsilon_2^*}{\mu_2}} \, E_0^2 \pi \sum_{n=1}^{\infty} \sum_{m=1}^{\infty} \frac{2n+1}{n(n+1)} \cdot \frac{2m+1}{m(m+1)} \cdot$$

$$\left\{ - |a_n^t|^2 \cdot \frac{S_n(k_2b)}{k_2b} \cdot \frac{S_m'(k_2b)^*}{k_2b^*} \cdot \int_{\theta=0}^{\pi} \frac{\partial P_n^1}{\partial \theta} \frac{\partial P_m^1}{\partial \theta} \sin \theta d\theta \right.$$

$$\left. + |b_n^t|^2 \cdot \frac{S_n'(k_2b)}{k_2b} \cdot \frac{S_m(k_2b)^*}{k_2b^*} \int_{\theta=0}^{\pi} \frac{P_n^1(\cos \theta)P_m^1(\cos \theta)}{\sin \theta} d\theta \right\} \qquad (12)$$

The Legendre functions have orthogonality properties which greatly simplify the expressions (Ref. 1, p. 417).

$$\int_0^{\pi} \left(\frac{\partial P_n^1}{\partial \theta} \cdot \frac{\partial P_m^1}{\partial \theta} + \frac{P_n^1 P_m^1}{\sin^2 \theta} \right) \sin \theta d\theta = \frac{2[n(n+1)]^2}{2n+1}, \quad m = n$$

$$= 0, \quad m \neq n \qquad (13)$$

Thus

$$\iint_{\Gamma} (S \cdot \hat{n}) da = - \frac{b^2}{2} \int_{\theta=0}^{\pi} \int_{\phi=0}^{2\pi} Re\{E_\theta H_\phi^* - E_\phi H_\theta^*\} \sin \theta d\theta d\phi$$

$$= j \sqrt{\frac{\epsilon_2^*}{\mu_2}} \frac{E_0^2 \pi}{|k_2|^2} \sum_{n=1}^{\infty} (2n+1) [- |a_n^t|^2 S_n(k_2b) S_n'(k_2b)^* + |b_n^t|^2 S_n'(k_2b) S_n(k_2b)^*] \qquad (14)$$

The power in the incident wave over an area πa^2 corresponds to the power passing through the area of the larger sphere if both spherical regions were composed of free space. The reference power is found by integrating the incident wave power density over a circular area πa^2.

$$P = \frac{1}{2} \cdot \pi a^2 \cdot Re\{\overline{E}_i \times \overline{H}_i^*\} \cdot \hat{a}_z$$

$$= \frac{\pi a^2}{2} \sqrt{\frac{\epsilon_0}{\mu_0}} E_0^2 \qquad (15)$$

If we let the inner medium be a lossy conductor, $\epsilon_2/\epsilon_0 = \epsilon' - j\epsilon''$, $\mu_2 = \mu_0$; the ratio of the absorbed power to the reference power is

10

$$j \, \frac{\sqrt{\epsilon' + j\epsilon''}}{|k_2 a|^2} \sum_{n=1}^{\infty} (2n+1) \left[|b_n^t|^2 S_n'(k_2 b) S_n(k_2 b)^* - |a_n^t|^2 S_n(k_2 b) S_n'(k_2 b)^* \right] \qquad (16)$$

2.2 SCATTERING OF A PLANE WAVE BY A LONG FERRITE CYLINDER

2.2.1 <u>Mathematical Analysis</u>.—The basic solution of this problem was outlined in Quarterly Report No. 4. Since then, the expressions for the Poynting vector inside and outside the cylinder, for TM and TE cases, have been formulated. In addition, expressions have been derived for the total power passing through a unit length of the cylinder. The fields and Poynting vector at the center of the cylinder have been evaluated on the IBM-704 and resonances noted for $\mu = \epsilon = 10$. The total power through the cylinder has been evaluated on the IBM-704 and resonances noted for several different values of μ and ϵ. The basic formulation of the problem is as follows.

<u>TM</u> <u>Case</u> (Fig. 4)

In addition to the expressions for the fields derived in Quarterly Progress Report No. 4, repeated below for convenience, expressions were derived for the Poynting vector and total power through the cylinder.

<u>Fields</u> (Ref. 1, p. 360)

<u>Fields Inside Cylinder</u>

$$E_Z = k^2 \sum_{n=-\infty}^{\infty} b_n e^{in\theta} J_n(kr)$$

$$H_r = \frac{k^2}{\mu \omega r} \sum_{n=-\infty}^{\infty} n b_n e^{in\theta} J_n(kr) \qquad (17)$$

$$H_\theta = \frac{ik^3}{\mu \omega} \sum_{n=-\infty}^{\infty} b_n e^{in\theta} J_n'(kr)$$

11

Fields Outside Cylinder

$$E_Z = k_0^2 \sum_{n=-\infty}^{\infty} a_n e^{in\theta} H_n^{(1)}(k_0 r) + A_0 \sum_{n=-\infty}^{\infty} J_n(k_0 r) e^{in\theta}$$

$$H_r = \frac{k_0^2}{\mu_0 \omega r} \sum_{n=-\infty}^{\infty} n a_n e^{in\theta} H_n^{(1)}(k_0 r) + A_0 \sqrt{\frac{\epsilon_0}{\mu_0}} \cos\theta \sum_{n=-\infty}^{\infty} J_n(k_0 r) e^{in\theta}$$

$$H_\theta = \frac{ik_0^3}{\mu_0 \omega} \sum_{n=-\infty}^{\infty} a_n e^{in\theta} H_n^{'(1)}(k_0 r) - A_0 \sqrt{\frac{\epsilon_0}{\mu_0}} \sin\theta \sum_{n=-\infty}^{\infty} J_n(k_0 r) e^{in\theta} \qquad (18)$$

Poynting Vectors

P_r Inside Cylinder at Point (r,θ)

$$P_r = -\frac{1}{2} \text{Re}(E_Z \times H_\theta^*)$$

$$P_r = -\frac{1}{2} \text{Re}\left[k^2 \sum_{n=-\infty}^{\infty} b_n e^{in\theta} J_n(kr)\right] \times \left[-\frac{ik^3}{\mu\omega} \sum_{n=-\infty}^{\infty} b_m^* e^{-im\theta} J_m'(kr)\right]$$

$$= \frac{1}{2} \text{Re} \frac{ik^5}{\mu\omega} \left[\sum_{n=-\infty}^{\infty} \sum_{m=-\infty}^{\infty} b_n b_m e^{i(n-m)\theta} J_n(kr) J_m'(kr)\right]$$

$$= -\frac{k^5}{2\mu\omega} \sum_{n=-\infty}^{\infty} \sum_{m=-\infty}^{\infty} J_n(kr) J_m'(kr) \left[(b_{nr}b_{mr} + b_{ni}b_{mi})\sin(n-m)\theta + \right.$$

$$\left. (b_{ni}b_{mr} - b_{nr}b_{mi})\cos(n-m)\theta\right] \qquad (19)$$

P_θ Inside Cylinder at Point (r,θ)

$$P_\theta = \frac{1}{2} \text{Re}(E_Z \times H_r^*) = \frac{1}{2} \text{Re}\left[k^2 \sum_{n=-\infty}^{\infty} b_n e^{in\theta} J_n(kr)\right]\left[\frac{k^2}{\mu\omega r} \sum_{m=-\infty}^{\infty} m b_m^* e^{im\theta} J_m(kr)\right]$$

$$= \frac{1}{2} \text{Re} \frac{k^4}{\mu\omega r} \left[\sum_{n=-\infty}^{\infty} \sum_{m=-\infty}^{\infty} m b_n b_m^* e^{i(n-m)\theta} J_n(kr) J_m(kr)\right]$$

$$= \frac{k^5}{2\mu\omega(kr)} \times \sum_{n=-\infty}^{\infty} \sum_{m=-\infty}^{\infty} m J_n(kr) J_m(kr) \left[(b_{nr}b_{mr} + b_{ni}b_{mi})\cos(n-m)\theta - \right.$$

$$\left. (b_{ni}b_{mr} - b_{nr}b_{mi})\sin(n-m)\theta\right] \qquad (20)$$

P_r Outside Cylinder at (r,θ)

$$P_r = -\frac{1}{2}\,\mathrm{Re}(E_Z \times H_\theta^*) = -\frac{1}{2}\,\mathrm{Re}\left[k_o^2\sum_{n=-\infty}^{\infty} a_n e^{in\theta} H_n^{(1)}(k_o r) + A_o \sum_{n=-\infty}^{\infty} J_n(k_o r)e^{in\theta}\right] \times \left[-\frac{ik_o^3}{\mu_o\omega}\sum_{m=-\infty}^{\infty} a_m^* e^{im\theta} H_m^{'(1)*}(k_o r)\right]$$

$$-A_o\sqrt{\frac{\epsilon_o}{\mu_o}}\,\sin\theta\sum_{m=-\infty}^{\infty} J_m(k_o r)e^{-im\theta}\Bigg] = -\frac{1}{2}\,\mathrm{Re}\left[-\frac{ik_o^5}{\mu_o\omega}\sum_{n=-\infty}^{\infty}\sum_{m=-\infty}^{\infty} a_n a_m^* H_n^{(1)}(k_o r) H_m^{'(1)*}(k_o r)e^{i(n-m)\theta}\right]$$

$$-\frac{A_o ik_o^3}{\mu_o\omega}\sum_{n=-\infty}^{\infty}\sum_{m=-\infty}^{\infty} a_m^* J_n(k_o r)H_m^{'(1)*}(k_o r)e^{i(n-m)\theta} - A_o k_o^2\sqrt{\frac{\epsilon_o}{\mu_o}}\,\sin\theta\sum_{n=-\infty}^{\infty}\sum_{m=-\infty}^{\infty} a_n J_m(k_o r)H_n^{(1)}(k_o r)e^{i(n-m)\theta}$$

$$-A_o^2\sqrt{\frac{\epsilon_o}{\mu_o}}\,\sin\theta\sum_{n=-\infty}^{\infty}\sum_{m=-\infty}^{\infty} J_n(k_o r)J_m(k_o r)e^{i(n-m)\theta}\Bigg]$$

substituting:

$$a_n = a_{nr} + i a_{ni}$$

$$H_n^{(1)} = J_n + iN_n \qquad \text{where } N_n = \text{Neumann function}$$

$$P_r = -\frac{k_o^5}{2\mu_o\omega}\sum_{n=-\infty}^{\infty}\sum_{m=-\infty}^{\infty}\Bigg\{\Big[(a_{nr}a_{mr}+a_{ni}a_{mi})\big(N_n(k_o r)J_m'(k_o r)-N_m'(k_o r)J_n(k_o r)\big)+(a_{ni}a_{mr}-a_{nr}a_{mi})\big(J_n(k_o r)J_m'(k_o r)$$

$$+N_n(k_o r)N_m'(k_o r)\big)\Big]\cos(n-m)\theta+\Big[(a_{nr}a_{mr}+a_{ni}a_{mi})\big(J_n(k_o r)J_m'(k_o r)+N_n(k_o r)N_m'(k_o r)\big)$$

$$-(a_{ni}a_{mr}-a_{nr}a_{mi})\big(N_n(k_o r)J_m'(k_o r)-N_m(k_o r)J_n'(k_o r)\big)\Big]\sin(n-m)\theta\Bigg\}-\frac{A_o k_o^3}{2\mu_o\omega}\sum_{n=-\infty}^{\infty}\sum_{m=-\infty}^{\infty}\Bigg[\Big(a_{mr}J_m'(k_o r)$$

$$-(a_{ni}J_m'(k_o r)+a_{mr}N_m'(k_o r)\big)\cos(n-m)\theta\times J_n(k_o r)-\big(a_{mi}J_m'(k_o r)+a_{mr}N_m'(k_o r)\big)\cos(n-m)\theta+\frac{A_o k_o^2}{2}\sqrt{\frac{\epsilon_o}{\mu_o}}\,\sin\theta\sum_{n=-\infty}^{\infty}\sum_{m=-\infty}^{\infty}$$

$$-a_{mi}N_m'(k_o r)\big)\sin(n-m)\theta\times J_n(k_o r)-\big(a_{nr}J_n(k_o r)-a_{ni}N_n(k_o r)\big)\cos(n-m)\theta+\frac{A_o^2}{2}\sqrt{\frac{\epsilon_o}{\mu_o}}\,\sin\theta\sum_{n=-\infty}^{\infty}\sum_{m=-\infty}^{\infty} J_n(k_o r)J_m(k_o r)\cos(n-m)\theta$$

$$\tag{21}$$

P_Θ Outside Cylinder at (r,Θ)

$$P_\Theta = \frac{1}{2}\text{Re}(E_Z \times H_r^*) = \frac{1}{2}\text{Re}\left[k_o^2 \sum_{n=-\infty}^{\infty} a_n e^{in\Theta} H_n^{(1)}(k_or) + A_o \sum_{n=-\infty}^{\infty} J_n(k_or)e^{in\Theta}\right] \times \left[\frac{k_o^2}{\mu_o\omega r}\sum_{m=-\infty}^{\infty} m a_m^* e^{-in\Theta} H_m^{(1)}(k_or)\right]$$

$$= \frac{1}{2}\text{Re}\left[\frac{k_o^4}{\mu_o\omega r}\sum_{n=-\infty}^{\infty}\sum_{m=-\infty}^{\infty} m a_m^* a_n J_m(k_or) e^{-im\Theta}\right]$$

$$+ A_o \sqrt{\frac{\epsilon_o}{\mu_o}}\cos\Theta\sum_{m=-\infty}^{\infty} J_m(k_or)e^{-im\Theta}$$

$$+ \frac{A_o k_o^2}{\mu_o\omega r}\sum_{n=-\infty}^{\infty}\sum_{m=-\infty}^{\infty} m a_m a_m^* J_n(k_or) H_m^{(1)}(k_or) e^{i(n-m)\Theta} + A_o k_o^2\sqrt{\frac{\epsilon_o}{\mu_o}}\cos\Theta\sum_{n=-\infty}^{\infty}\sum_{m=-\infty}^{\infty} a_n a_m^* m J_n(k_or) H_m^{(1)}{}^*(k_or) e^{i(n-m)\Theta} + A_o k_o^2\sqrt{\frac{\epsilon_o}{\mu_o}}\cos\Theta\sum_{n=-\infty}^{\infty}\sum_{m=-\infty}^{\infty} a_n J_m(k_or) H_n^{(1)}(k_or) e^{i(n-m)\Theta}$$

$$+ A_o^2\sqrt{\frac{\epsilon_o}{\mu_o}}\cos\Theta\sum_{n=-\infty}^{\infty}\sum_{m=-\infty}^{\infty} J_n(k_or) J_m(k_or) e^{i(n-m)\Theta} = \frac{k_o^4}{\mu_o\omega r}\sum_{n=-\infty}^{\infty}\sum_{m=-\infty}^{\infty}\left[\left(a_{nr}a_{mr} + a_{ni}a_{mi}\right)\left(J_n(k_or) J_m(k_or)\right)\right.$$

$$+ N_n(k_or)N_m(k_or)) - \left(a_{ni}a_{mr} - a_{mi}a_{nr}\right)\left(J_m(k_or)N_n(k_or) - J_n(k_or)N_m(k_or)\right)\right] \times \cos(n-m)\Theta - \left[\left(a_{ni}a_{mr} - a_{mi}a_{nr}\right)\right.$$

$$\left(J_n(k_or) J_m(k_or) + N_n(k_or)N_m(k_or)\right) + \left(a_{nr}a_{mr} + a_{ni}a_{mi}\right)\left(J_m(k_or)N_n(k_or) - J_n(k_or)N_m(k_or)\right)\right] \times \sin(n-m)\Theta$$

$$+ \frac{A_o k_o^2}{2\mu_o\omega r}\sum_{n=-\infty}^{\infty}\sum_{m=-\infty}^{\infty}\left\{\left[a_{mr}J_m(k_or) + a_{mi}J_m(k_or)\right]\cos(n-m)\Theta + \left[a_{mi}J_m(k_or) + a_{mr}N_m(k_or)\right]\sin(n-m)\Theta\right\}J_n(k_or)$$

$$+ \frac{A_o k_o^2}{2}\sqrt{\frac{\epsilon_o}{\mu_o}}\cos\Theta\sum_{n=-\infty}^{\infty}\sum_{m=-\infty}^{\infty}\left[\left(a_{nr}J_n(k_or) - a_{ni}N_n(k_or)\right)\cos(n-m)\Theta - \left(a_{ni}J_n(k_or) + a_{nr}N_n(k_or)\right)\sin(n-m)\Theta\right]J_m(k_or)$$

$$+ \frac{A_o^2}{2}\sqrt{\frac{\epsilon_o}{\mu_o}}\cos\Theta\sum_{n=-\infty}^{\infty}\sum_{m=-\infty}^{\infty} J_n(k_or)J_m(k_or)\cos(n-m)\Theta \qquad (22)$$

Total Power Passing Through Unit Length of Cylinder

Total power $= \int_0^1 \int_0^\pi a P_r d\Theta d\ell = a \int_0^\pi P_r d\Theta$ (radius of cylinder = a)

$$= \frac{-k^5 a}{2\mu\omega} \int_0^\pi \sum_{n=-\infty}^{\infty} \sum_{m=-\infty}^{\infty} \left[(b_{nr}b_{mr} + b_{ni}b_{mi}) \sin(n-m)\Theta + (b_{ni}b_{mr} - b_{nr}b_{mi}) \cos(n-m)\Theta \right]$$

$$J_n(kr) J_m^!(kr) \times d\Theta$$

$$= -\frac{k^5 a}{2\mu\omega} \sum_{n=-\infty}^{\infty} \sum_{m=-\infty}^{\infty} J_n(ka) J_m^!(ka) \left[(b_{nr}b_{mr} + b_{ni}b_{mi}) \int_0^\pi \sin(n-m)\Theta d\Theta \right.$$

$$\left. + (b_{ni}b_{mr} - b_{nr}b_{mi}) \int_0^\pi \cos(n-m)\Theta d\Theta \right]$$

$$= -\frac{k^5 a}{2\mu\omega} \sum_{n=-\infty}^{\infty} \sum_{m=-\infty}^{\infty} J_n(ka) J_m^!(ka)(b_{nr}b_{mr} + b_{ni}b_{mi}) \times \left[\frac{(-1)^{n-m}-1}{n-m} \right]$$ (contribution only when n+m is odd)

Changing Summation to (0 to ∞)

$$= -\frac{ak^5}{\mu\omega} \times \sum_0^\infty \sum_0^\infty \frac{\epsilon_{on}\epsilon_{om}}{} J_n(ka) J_m^!(ka) \frac{(b_{nr}b_{mr}+b_{ni}b_{mi})n}{n^2 - m^2}$$ (for m even, n odd)

$$(23)$$

$$- \frac{ak^5}{\mu\omega} \sum_0^\infty \sum_0^\infty \frac{\epsilon_{on}\epsilon_{om}}{} J_n(ka) J_m^!(ka) \frac{(b_{nr}b_{mr}+b_{ni}b_{mi})m}{n^2 - m^2}$$ (for n even, m odd)

Power through same area in free space

$$= A_0^2 \sqrt{\frac{\epsilon_0}{\mu_0}} \times a$$

$$(24)$$

Dividing Eq. (23) by (24) gives the ratio of power through the cylinder to the power through the same cross-sectional area.

$$\epsilon_{on} = 1 \ (n = 0)$$

$$= 2 \ (n \neq 0)$$

15

In the above, a_{nr}, a_{ni}, b_{nr}, b_{ni} for the TM case are defined as follows:

$$a_n = a_{nr} + ia_{ni} = -\frac{A_o}{k_o^2} \times \frac{[\alpha J_n(ka) J_n'(k_oa) - J_n(k_oa) J_n'(ka)]}{[\alpha H_n'^{(1)}(k_oa) J_n(ka) - H_n^{(1)}(k_oa) J_n'(ka)]}$$

(25)

$$b_n = b_{nr} + ib_{ni} = \frac{\alpha A_o}{k^2} \frac{[H_n'^{(1)}(k_oa) J_n(k_oa) - H_n^{(1)}(k_oa) J_n'(k_oa)]}{[\alpha H_n'^{(1)}(k_oa) J_n(ka) - H_n^{(1)}(k_oa) J_n'(ka)]}$$

where

$$\alpha = \neg \sqrt{\frac{\mu \epsilon_o}{\mu_o \epsilon}}, \quad k_o = \omega \sqrt{\mu_o \epsilon_o}, \quad k = \omega \sqrt{\mu \epsilon}$$

$$H_n'^{(1)}(k_oa) J_n(k_oa) - H_n^{(1)}(k_oa) J_n'(k_oa) = \frac{2i}{\pi k_oa} \quad \text{(by Wronskian relationship)}.$$

Primes denote differentiation with respect to argument.

$$a_{nr} = \frac{A_o}{k_o^2} \times \frac{[\alpha J_n(ka) J_n'(k_oa) - J_n(k_oa) J_n'(ka)][\alpha J_n'(k_oa) J_n(ka) - J_n(k_oa) J_n'(ka)]}{D_n}$$

$$a_{ni} = -\frac{A_o}{k_o^2} \frac{[\alpha J_n(ka) J_n'(k_oa) - J_n(k_oa) J_n'(ka)][\alpha N_n'(k_oa) J_n(ka) - N_n(k_oa) J_n'(ka)]}{D_n}$$

$$b_{nr} = -\frac{2\alpha A_o}{\pi k^2 k_oa} \times \frac{[N_n(k_oa) J_n'(ka) - \alpha N_n'(k_oa) J_n(ka)]}{D_n}$$

$$b_{ni} = -\frac{2\alpha A_o}{\pi k^2 k_oa} \times \frac{[J_n(k_oa) J_n'(ka) - \alpha J_n'(k_oa) J_n(ka)]}{D_n}$$

(26)

where D_n (TM case)

$$= [\alpha J_n'(k_oa) J_n(ka) - J_n(k_oa) J_n'(ka)]^2$$
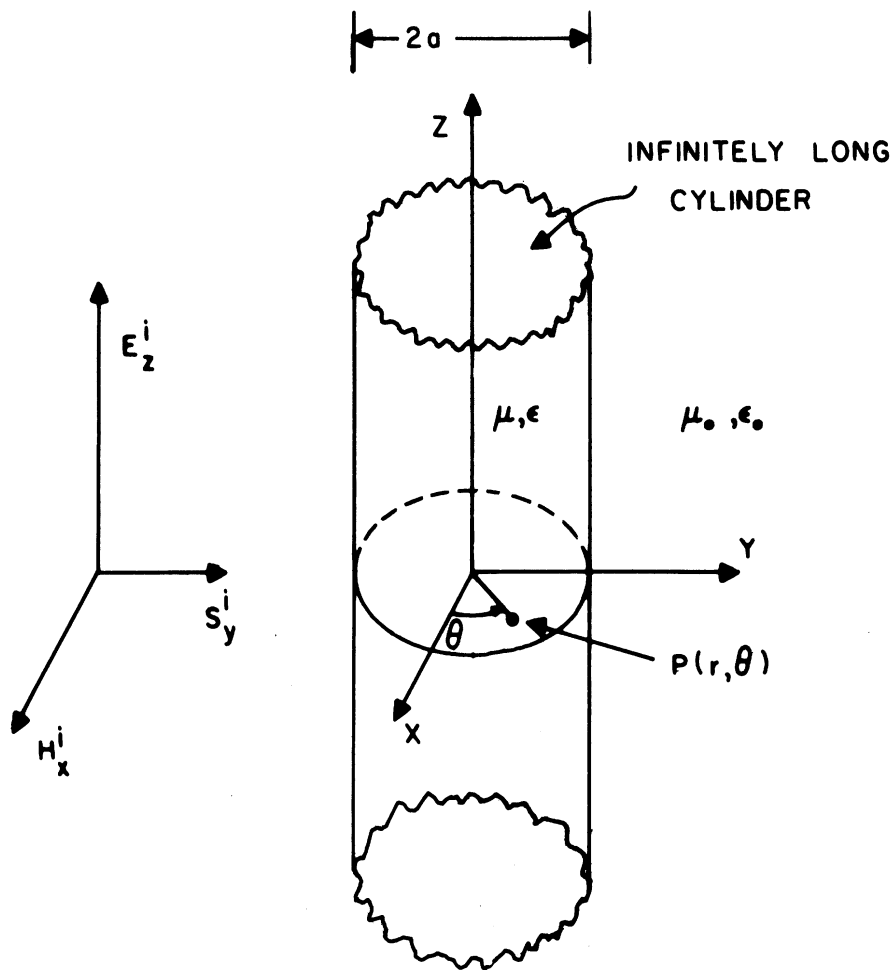
$$+ [\alpha N_n'(k_oa) J_n(ka) - N_n(k_oa) J_n'(ka)]^2$$

16

Fig. 4. Plane wave incident on cylinder, electric field parallel to cylinder axis.

As in the TM case, expressions were derived for fields, Poynting vector, and total power through the cylinder.

Fields (Ref. 1, p. 360)

Fields Inside Cylinder

$$H_Z = k^2 \sum_{n=-\infty}^{\infty} b_n e^{in\theta} J_n(kr)$$

$$E_r = -\frac{\mu\omega}{r} \sum_{n=-\infty}^{\infty} n b_n e^{in\theta} J_n(kr) \qquad (27)$$

$$E_\theta = -ik\mu\omega \sum_{n=-\infty}^{\infty} b_n e^{in\theta} J_n'(kr)$$

Fields Outside Cylinder

$$H_Z = k_0^2 \sum_{n=-\infty}^{\infty} a_n e^{in\theta} H_n^{(1)}(k_0 a) + A_0 \sqrt{\frac{\epsilon_0}{\mu_0}} \sum_{n=-\infty}^{\infty} e^{in\theta} J_n(k_0 r)$$

$$E_r = \frac{\mu_0\omega}{r} \sum_{n=-\infty}^{\infty} n a_n e^{in\theta} H_n^{(1)}(k_0 a) + A_0 \cos\theta \sum_{n=-\infty}^{\infty} e^{in\theta} J_n(k_0 r) \qquad (28)$$

$$E_\theta = -ik_0\mu_0\omega \sum_{n=-\infty}^{\infty} a_n e^{in\theta} H_n'^{(1)}(k_0 a) - A_0 \sin\theta \sum_{n=-\infty}^{\infty} e^{in\theta} J_n(k_0 r)$$

Poynting Vectors

P_r Inside Cylinder at Point (r,θ)

$$P_r = \frac{1}{2} \text{Re}(E_\theta \times H_Z^*) = \frac{1}{2} \text{Re}\left[-ik\mu\omega \sum_{n=-\infty}^{\infty} b_n e^{in\theta} J_n'(kr)\right]\left[k^2 \sum_{m=-\infty}^{\infty} b_m^* e^{im\theta} J_m(kr)\right]$$

$$= \frac{1}{2} \text{Re}\left[-ik^3\mu\omega \sum_{n=-\infty}^{\infty} \sum_{m=-\infty}^{\infty} b_n b_m^* e^{i(n-m)\theta} J_n'(kr) J_m(kr)\right]$$

$$= \frac{k^3\mu\omega}{2} \sum_{n=-\infty}^{\infty} \sum_{m=-\infty}^{\infty} \left[(b_{nr}b_{mr} + b_{ni}b_{mi})\sin(n-m)\theta\right.$$

$$\left. + (b_{ni}b_{mr} - b_{nr}b_{mi})\cos(n-m)\theta\right] \times J_m(kr) J_n'(kr) \qquad (29)$$

P_θ Inside Cylinder at Point (r,θ)

$$P_\theta = -\frac{1}{2}\text{Re}(E_r \times H_z^*) = -\frac{1}{2}\text{Re}\left[-\frac{\mu\omega}{r}\sum_{n=-\infty}^{\infty}nb_ne^{in\theta}J_n(kr)\right]\left[k^2\sum_{m=-\infty}^{\infty}b_m^*e^{-im\theta}J_m(kr)\right] = \text{Re}\frac{\mu\omega}{2r}\sum_{n=-\infty}^{\infty}\sum_{m=-\infty}^{\infty}nb_nb_m^*e^{i(n-m)\theta}J_n(kr)J_m(kr)$$

$$= \frac{\mu\omega}{2r}\sum_{n=-\infty}^{\infty}\sum_{m=-\infty}^{\infty}nJ_n(kr)J_m(kr)\left[(b_{nr}b_{mr}+b_{ni}b_{mi})\cos(n-m)\theta - (b_{ni}b_{mr} - b_{nr}b_{mi})\sin(n-m)\theta\right]$$

P_r Outside Cylinder at Point (r,θ)

$$P_r = \frac{1}{2}\text{Re}(E_\theta \times H_z^*) = \frac{1}{2}\text{Re}\left[-i\mu_0\omega k_0\sum_{n=-\infty}^{\infty}a_ne^{in\theta}H_n^{(1)\prime}(k_0r) - A_0\sin\theta\sum_{n=-\infty}^{\infty}e^{in\theta}J_n(k_0r)\right]\times\left[k_0^2\sum_{m=-\infty}^{\infty}a_m^*e^{-im\theta}H_m^{(1)*}(k_0r)\right]$$

$$+ A_0\sqrt{\frac{\epsilon_0}{\mu_0}}\sum_{m=-\infty}^{\infty}e^{-im\theta}J_m(k_0r)\right] = \frac{1}{2}\text{Re}\left\{-i\mu_0\omega k_0^3\sum_{n=-\infty}^{\infty}\sum_{m=-\infty}^{\infty}a_na_m^*H_n^{(1)\prime}(k_0r)H_m^{(1)*}(k_0r)e^{i(n-m)\theta}\right.$$

$$- A_0k_0^2\sin\theta\sum_{n=-\infty}^{\infty}\sum_{m=-\infty}^{\infty}a_m^*J_n(k_0r)H_m^{(1)*}(k_0r)e^{i(n-m)\theta} - iA_0\mu_0\omega k_0\sqrt{\frac{\epsilon_0}{\mu_0}}\sum_{n=-\infty}^{\infty}\sum_{m=-\infty}^{\infty}a_nJ_m(k_0r)H_n^{(1)\prime}(k_0r)e^{i(n-m)\theta}$$

$$- A_0^2\sqrt{\frac{\epsilon_0}{\mu_0}}\sin\theta\sum_{n=-\infty}^{\infty}\sum_{m=-\infty}^{\infty}J_n(k_0r)J_m(k_0r)e^{i(n-m)\theta}\right\}$$

$$= \frac{\mu_0\omega k_0^3}{2}\sqrt{\frac{\mu_0\omega k_0^3}{}}\sum_{n=-\infty}^{\infty}\sum_{m=-\infty}^{\infty}\left[\left((a_{nr}a_{mr}+a_{ni}a_{mi})J_n^\prime(k_0r)J_m(k_0r) + N_m^\prime(k_0r)N_n(k_0r)\right) - (a_{ni}a_{mr} - a_{nr}a_{mi})(N_m^\prime(k_0r)J_m(k_0r) - N_m(k_0r)J_n^\prime(k_0r))\right]\cos(n-m)\theta$$

$$\sin(n-m)\theta + \left((a_{ni}a_{mr} - a_{nr}a_{mi})(J_n^\prime(k_0r)J_m(k_0r) + N_n^\prime(k_0r)N_m(k_0r)) + (a_{nr}a_{mr} + a_{ni}a_{mi})(N_n^\prime(k_0r)J_m(k_0r) - N_m(k_0r)J_n^\prime(k_0r))\right)\sin(n-m)\theta\right] + \frac{A_0k_0^2}{2}\sum_{n=-\infty}^{\infty}\sum_{m=-\infty}^{\infty}J_n(k_0r)J_m(k_0r)\cos(n-m)\theta$$

$$- \frac{A_0k_0^2\sin\theta}{2}\sum_{n=-\infty}^{\infty}\sum_{m=-\infty}^{\infty}\left[\left((a_{mr}J_m(k_0r) - a_{mi}N_m(k_0r))\cos(n-m)\theta + (a_{mi}J_m(k_0r) + a_{mr}N_m(k_0r))\sin(n-m)\theta\right)J_m(k_0r)\right] - \frac{A_0^2}{2}\sqrt{\frac{\epsilon_0}{\mu_0}}\sin\theta\sum_{n=-\infty}^{\infty}\sum_{m=-\infty}^{\infty}J_n(k_0r)J_m(k_0r)\cos(n-m)\theta$$

$$- a_{ni}N_n^\prime(k_0r))\sin(n-m)\theta + (a_{ni}J_n^\prime(k_0r) + a_{nr}N_n^\prime(k_0r))\cos(n-m)\theta$$

$$\tag{31}$$

19

$\underline{P_\theta}$ $\underline{\text{Outside}}$ $\underline{\text{Cylinder}}$ $\underline{\text{at}}$ $\underline{\text{Point}}$ $\underline{(r,\theta)}$

$$P_\theta = -\frac{1}{2}\,\mathrm{Re}(E_r \times H_z^*) = -\frac{1}{2}\,\mathrm{Re}\left[\frac{\mu_0\omega}{r}\left(\sum_{n=-\infty}^{\infty} na_n e^{in\theta}H_n^{(1)}(k_o r) + A_o\cos\theta\sum_{n=-\infty}^{\infty} e^{in\theta}J_n(k_o r)\right) \times \left[k_o^2\sum_{m=-\infty}^{\infty} a_m^* e^{-im\theta}H_m^{(1)*}(k_o r)\right]\right.$$

$$+ A_o - \sqrt{\frac{\epsilon_o}{\mu_o}}\sum_{m=-\infty}^{\infty} e^{-im\theta}J_m(k_o r)\right] = \frac{1}{2}\,\mathrm{Re}\left\{-\frac{\mu_o\omega k_o^2}{r}\sum_{n=-\infty}^{\infty}\sum_{m=-\infty}^{\infty} na_n a_m^* e^{i(n-m)\theta}H_n^{(1)}(k_o r)H_m^{(1)*}(k_o r)\right.$$

$$- A_o k_o^2\cos\theta\sum_{n=-\infty}^{\infty}\sum_{m=-\infty}^{\infty} a_m^* H_m^{(1)*}(k_o r)e^{i(n-m)\theta}J_n(k_o r) - A_o\sqrt{\frac{\epsilon_o}{\mu_o}} \times \frac{\mu_o\omega}{r}\sum_{n=-\infty}^{\infty}\sum_{m=-\infty}^{\infty} na_n e^{i(n-m)\theta}H_n^{(1)}(k_o r)J_m(k_o r)$$

$$- A_o^2\sqrt{\frac{\epsilon_o}{\mu_o}}\cos\theta\sum_{n=-\infty}^{\infty}\sum_{m=-\infty}^{\infty} J_n(k_o r)J_m(k_o r)e^{i(n-m)\theta}e^{i(n-m)\theta}\right\}$$

$$= \left\{-\frac{\mu_o\omega k_o^2}{2r}\sum_{n=-\infty}^{\infty}\sum_{m=-\infty}^{\infty}\left[\left(a_{nr}a_{mr} + a_{ni}a_{mi}\right)\left(J_n(k_o r)J_m(k_o r) + N_n(k_o r)N_m(k_o r)\right) - \left(a_{ni}a_{mr} - a_{mi}a_{nr}\right)\left(J_m(k_o r)N_n(k_o r)\right.\right.\right.$$

$$\left. - J_n(k_o r)N_m(k_o r)\right) + \left(a_{ni}a_{mr} - a_{mi}a_{nr}\right)\Big]\cos(n-m)\theta - \Big[\left(a_{nr}a_{mr} + a_{ni}a_{mi}\right)\left(J_n(k_o r)N_m(k_o r)\right.$$

$$\left. - J_n(k_o r)N_m(k_o r)\right)\Big]\cos(n-m)\theta\right) - \frac{A_o k_o^2\cos\theta}{2}\sum_{n=-\infty}^{\infty}\sum_{m=-\infty}^{\infty}\left[\left(a_{mr}J_m(k_o r) - a_{mi}N_m(k_o r)\right)\cos(n-m)\theta\right.$$

$$\left. - \left(J_n(k_o r)J_m(k_o r) + N_n(k_o r)N_m(k_o r)\right)\sin(n-m)\theta\right]n - \frac{A_o k_o}{2r}\sum_{n=-\infty}^{\infty}\sum_{m=-\infty}^{\infty}\left[\left(a_{nr}J_n(k_o r) - a_{ni}N_n(k_o r)\right)\cos(n-m)\theta\right.$$

$$\left. - \left(a_{mi}J_m(k_o r) + a_{mr}N_m(k_o r)\right)\sin(n-m)\theta\right]J_n(k_o r) - A_o^2\sqrt{\frac{\epsilon_o}{\mu_o}}\cos\theta\sum_{n=-\infty}^{\infty}\sum_{m=-\infty}^{\infty} nJ_m(k_o r)$$

$$- \left(a_{ni}J_n(k_o r) + a_{nr}N_n(k_o r)\right)\sin(n-m)\theta\;J_n(k_o r)J_m(k_o r)\cos(n-m)\theta\right\}$$

Total Power Passing Through Unit Length of Cylinder

Total power $= \int_0^1 \int_0^\pi a P_r \, d\Theta d\ell$ (a = radius of cylinder)

$$= \frac{k^3 \mu \omega}{2} \sum_{n=-\infty}^{\infty} \sum_{m=-\infty}^{\infty} J_m(ka) J_n'(ka) \left[(b_{nr}b_{mr} + b_{ni}b_{mi}) \int_0^\pi \sin(n-m)\Theta d\Theta \right.$$

$$\left. + (b_{ni}b_{mr} - b_{nr}b_{mi}) \int_0^\pi \cos(n-m)\Theta d\Theta \right]$$

$$= \frac{k^3 \mu \omega}{2} \sum_{n=-\infty}^{\infty} \sum_{m=-\infty}^{\infty} J_m(ka) J_n'(ka) (b_{nr}b_{mr} + b_{ni}b_{mi}) \frac{[(-1)^{n-m} - 1]}{n-m}$$ (contribution only when n+m odd)

Changing Summation to (0 to ∞)

Total power

$$= - \frac{k^3 \mu \omega}{2} \sum_{n=0}^{\infty} \sum_{m=0}^{\infty} J_n(ka) J_m'(ka) \frac{(b_{nr}b_{mr} + b_{ni}b_{mi})n}{n^2 - m^2} \epsilon_{on}\epsilon_{om} \text{ (for m even, n odd)}$$

$$- \frac{k^3 \mu \omega}{2} \sum_{n=0}^{\infty} \sum_{m=0}^{\infty} J_n(ka) J_m'(ka) \frac{(b_{nr}b_{mr} + b_{ni}b_{mi})m}{n^2 - m^2} \epsilon_{on}\epsilon_{om} \text{ (for n even, m odd)}$$

$$\tag{33}$$

Power through same area in free space

$$= A_0^2 \sqrt{\frac{\epsilon_0}{\mu_0}} \times a. \tag{33a}$$

Dividing Eq. (33) by (33a) gives the ratio of power through cylinder to the power through the same area in free space.

In the above, a_{nr}, a_{mr}, b_{nr}, b_{ni} for the TE case are defined as follows:

$$a_n = -\frac{A_o}{k_o^2}\sqrt{\frac{\epsilon_o}{\mu_o}} \; \frac{[\alpha J_n(k_{oa}) J_n'(ka) + J_n(ka) J_n'(k_{oa})]}{[\alpha H_n(k_{oa}) J_n'(ka) - H_n'(k_{oa}) J_n(ka)]}$$

$$b_n = -\frac{A_o}{k^2}\sqrt{\frac{\epsilon_o}{\mu_o}} \; \frac{[H_n(k_{oa}) J_n'(ka) + J_n(k_{oa}) H_n'(k_{oa})]}{[\alpha H_n(k_{oa}) J_n'(ka) - H_n'(k_{oa}) J_n(ka)]} \qquad (34)$$

$$a_{nr} = -\frac{A_o}{k_o^2}\sqrt{\frac{\epsilon_o}{\mu_o}} \; \frac{[\alpha J_n(k_{oa}) J_n'(ka) + J_n(ka) J_n'(k_{oa})][\alpha J_n'(ka) J_n(k_{oa}) - J_n(ka) J_n'(k_{oa})]}{D_n}$$

$$a_{ni} = \frac{A_o}{k_o^2}\sqrt{\frac{\epsilon_o}{\mu_o}} \; \frac{[\alpha J_n(k_{oa}) J_n'(ka) + J_n(ka) J_n'(k_{oa})][\alpha J_n'(ka) N_n(k_{oa}) - J_n(ka) N_n'(k_{oa})]}{D_n}$$

$$b_{nr} = -\frac{A_o}{k^2}\sqrt{\frac{\epsilon_o}{\mu_o}} \; \frac{[2J_n'(k_{oa}) J_n(k_{oa})][\alpha J_n'(ka) J_n(k_{oa}) - J_n(ka) J_n'(k_{oa})] + [J_n'(k_{oa}) N_n(k_{oa}) + J_n(k_{oa}) N_n'(k_{oa})][\alpha J_n'(ka) N_n(k_{oa}) - J_n(ka) N_n'(k_{oa})]}{D_n}$$

$$b_{ni} = +\frac{A_o}{k^2}\sqrt{\frac{\epsilon_o}{\mu_o}} \; \frac{[2J_n'(k_{oa}) J_n(k_{oa})][\alpha J_n'(ka) N_n(k_{oa}) - J_n(ka) N_n'(k_{oa})] - [J_n'(k_{oa}) J_n(k_{oa})][\alpha J_n'(ka) J_n(k_{oa}) + J_n(k_{oa}) N_n'(k_{oa})]}{D_n}$$

where D_n(TE case)

$$= [\alpha J_n'(ka) J_n(k_{oa}) - J_n(ka) J_n'(k_{oa})]^2 + [\alpha J_n'(ka) N_n(k_{oa}) - J_n(ka) N_n'(k_{oa})]^2 \qquad (35)$$
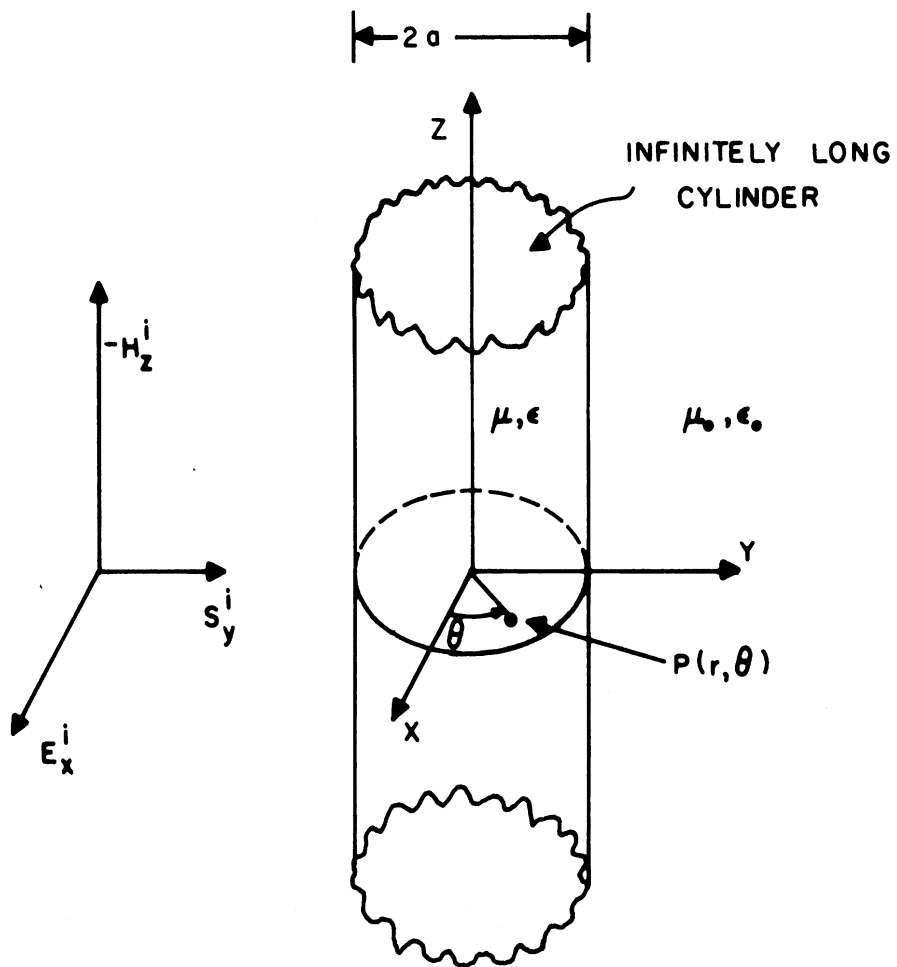
Fig. 5. Plane wave incident on cylinder, electric field perpendicular to cylinder axis.

2.2.2 Computer Results—Interpretation of the Resonance Properties

Shown by the Total Power Flow Through a Unit Length of Cylindrical Ferrite

and Dielectric Material (TM Case).—The results of a computer study show-

ing the normalized power flowing through a unit length of a lossless ferrite

or dielectric cylinder with an incident plane wave appear in Figs. 6-9. The

normalized power is defined as the ratio of the power flowing through the

front surface of the cylinder (subtending an arc of 180° at the center of

the circular cross section) with the material medium present to the power

that would pass through the sam cross-sectional area in free space. There-

fore, whenever the magnitude of the normalized power level exceeds one,

there is more energy flowing into or out of a unit length of the cylinder

than would pass through the same area in free space.

Before the graphs are described in detail, some remarks on their gen-

eral behavior might be in order. The expectation entertained before any

numerical computations were performed was that the cylinder should exhibit

transverse model resonances at well-defined frequencies, depending on the

propagation characteristics. Since, in the building of any practical an-

tenna structure utilizing the energy densities available inside the cyl-

inder, it will be important to know the total energy flow into the cylinder

rather than that computed on the basis of a few modes, it was decided to

compute several final plots for the total normalized power flow into the

cylinder. It was hoped that these plots of power flow would still show an

improvement or resonance condition even though taking the integral over the

front surface of the cylinder involves an averaging process which should

PERCENTAGES = $\dfrac{\text{BANDWIDTH FOR }|\text{NORMALIZED POWER}| > 1}{\text{CENTER FREQUENCY OF RESONANCE}}$

Fig. 6. Power flow through the cross section of a long ferrite cylinder.

$\mu = 3$
$\epsilon = 3$

NORMALIZED POWER

$a/\lambda_f \longrightarrow$

25

Fig. 7. Power flow through the cross section of a long ferrite cylinder.
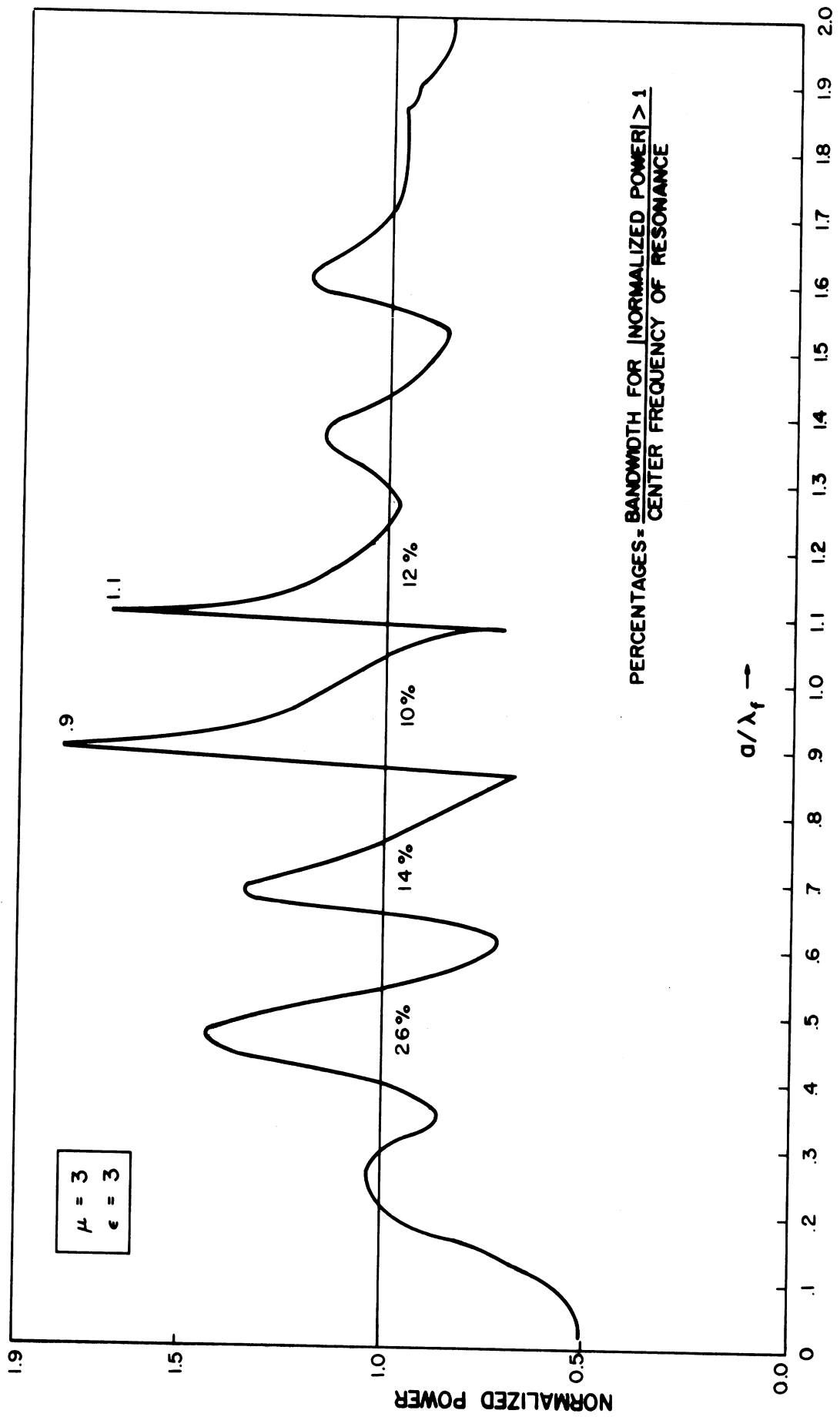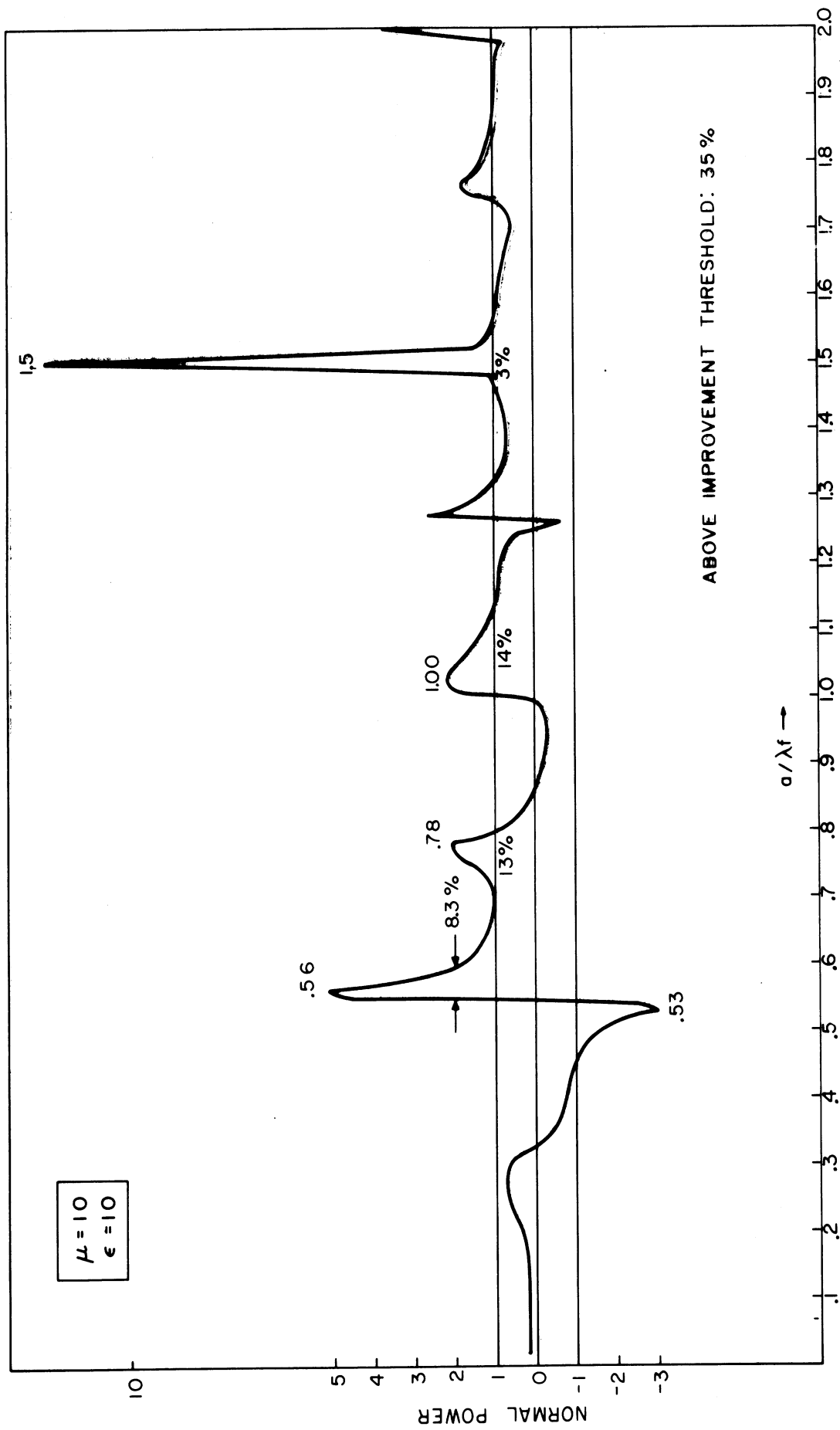
26

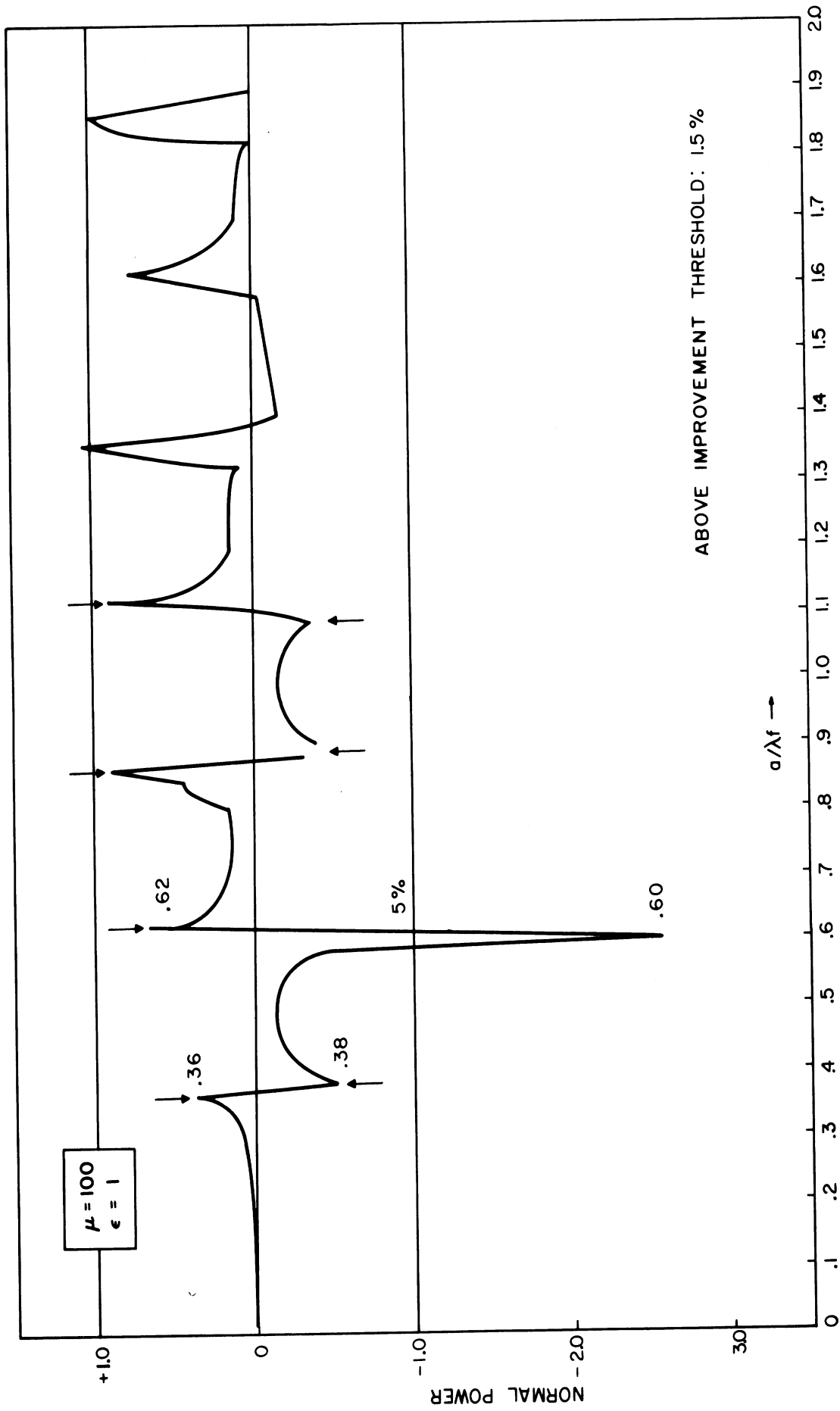Fig. 8. Power flow through the cross section of a long dielectric cylinder.

Fig. 9. Power flow through the cross section of a long ferrite cylinder.

cut down the resonance peaks considerably. In addition to this averaging, there is a large amount of mismatch that will confront the incoming plane wave whenever the characteristic impedance of the cylinder is very much different from that of the surrounding free space, i.e., when $\sqrt{\mu/\epsilon}$ is much different from 377 ohms. In two figures, Figs. 6 and 7, Z_O is that of free space. In Figs. 8 and 9 Z_O is 37.7 and 3770 ohms, respectively. Both of these impedances would give rise to a reflection coefficient of $\pm$ .8 for a plane wave meeting a plane boundary. While the effect for a curved boundary is harder to predict, it is safe to say that this change of characteristic impedance will introduce a mismatch in fields at the boundary leading to a loss in the energy densities penetrating inside the body.

Because of the difference in characteristic impedance it is natural to discuss the four graphs in two groups. Figures 6 and 7, for $\mu = \epsilon = 3$ and $\mu = \epsilon = 10$, respectively, have $Z_O = 1$. Figures 8 and 9, $\mu = 1$, $\epsilon = 100$, and $\mu = 100$, $\epsilon = 1$, have $Z_O = .1$ and $Z_O = 10$, respectively.

In the first two figures it can be observed that the value of the permeability and the permittivity has a profound influence upon the shape of the power resonance curve. In the first place, the low frequency value of the total power in the cylinder, i.e., the value for a thin cylinder, reaches .5 for Fig. 6 ($\mu = \epsilon = 3$) and .2 for Fig. 7 ($\mu = \epsilon = 10$).

In case I the first resonance is reached at approximately $a = .25\lambda_{ferrite}$. All the resonances evident, up to the one at $a = 1.6\lambda_f$ occur spaced .21-.24 ferrite wavelengths apart. This is quite an amazing regularity, considering that terms from which the coefficients of the separate modes are derived

exhibit resonances due to the difference in the denominator of properly

weighted products of Bessel and Hankel functions. Therefore, for the indi-

vidual modes we would certainly not expect this regularity evident in the

average power flow into the cylinder. All the resonances occurring are fairly

broad, reaching bandwidths between 26% (at $.5\lambda_f$) and 12% (at $1.1\lambda_f$) of the

center frequency. For all the following discussion, bandwidth will be defined

as that region of frequency over which the absolute value of the normalized

power flow into the cylinder reaches a value larger than one. This bandwidth

is indicated for each peak on the graphs. All the resonances which occur

are of moderate height, with the highest peak reached equal to 1.8. A fea-

ture which distinguishes case I from all the other cases is quite significant.

For $\mu = \epsilon = 3$, the only resonances obtained are _positive_ values, i.e., the

normalized power oscillates about the +1 line, never reaching -1 (or any neg-

ative value). This is significant because it means that, up to a radius a =

$2\lambda_f$ (at least), power always flows _into_ the front half of the cylinder; never

does power flow out of it. For all the other computed cases there occur both

plus and minus resonances, signifying that there is a net power flow both

into and out of the front half of the cylinder.

Figure 7, $\mu = \epsilon = 10$, presents quite a different picture. Note the

change of scale which was necessary to portray accurately the shape of each

of the four graphs. This is the only case in which there is not a large

amount of periodicity in the resonance peaks. One phenomenon typical of Figs.

8 and 9 is demonstrated by the twin resonance at .53 and $.56\lambda_f$ (of magnitude

3 and 5, respectively). Between these two points, with a 6% change in fre-

quency, the flow of power is reversed in direction. This change in the direction of power flow could be used in an antenna system to obtain some quite selective filtering of two slightly different frequencies. For this case peaks of magnitude 2 and bandwidths of over 10% are reached several times (at .78λ_f and 1.02λ_f). Narrower twin resonances occur in the neighborhood of .55λ_f and 1.27λ_f. A narrow resonance of 3% bandwidth and peak value of 12 is found at 1.5λ_f. This is the highest power concentration found in the entire graph, and oddly enough it does not have minus resonance point associated with it.

Figure 8 depicts the case μ = 1, ϵ = 100. The first impression the viewer gets from this graph is one of resonance peaks rising at quite regular intervals. Indeed, all the resonances from .62λ_f on up occur at .25-wavelength intervals. These resonances are quite narrow (2-5%), reaching peaks between 1.5 and 2.3. All peaks are positive. The lower frequency behavior is quite interesting. At .36 and .38 a narrow twin resonance occurs, 6% and 12% in bandwidth, with the positive peak reaching up to 9. At the very low frequency end, it is seen that, in this particular case, there is resonance right from the lowest frequency until the radius of the rod reaches .12λ_f. The concentration of power is not very outstanding; however, both bandwidth of operation and the physical shape of the setup (we require only a thin rod, instead of the heavier ones needed for higher-order resonances) are quite attractive.

For Fig. 9, μ = 100, and ϵ = 1, the computer increments in a/λ_f were not small enough. Even though a computation was made for every .02 increment in a/λ_f, it is apparent that most of the resonance peaks were missed. The

neighborhood of the resonances which appear will have to be explored with more care. Even though there is only one actual computed point which definitely shows resonance (at $a = .60\lambda_f$), it still can be seen that there are other resonances also. All of them appear quite narrow, with bandwidths of 2% or less. Without any computer points of high value, it is of course impossible to say how high the peak values of the resonance curves are. Once more, several of these resonances are spaced about $.25\lambda_f$ apart. One disadvantage of this high permeability case would be presented by its low-frequency behavior; for thin cylinders up to about $.3\lambda_f$ in radius, the normalized power is much less than one. From a practical standpoint, then, this configuration would be less desirable than case III since a much bulkier cylinder would be required to obtain resonance. In all the graphs shown, the peaks have not been examined in detail and could conceivably rise to higher values than those shown on the graphs.

2.3 SCATTERING OF A PLANE WAVE BY A FERRITE PROLATE SPHEROID

An investigation of plane-wave scattering by a prolate spheroid was initiated. This study was planned as an extension of the ferrite-cylinder and ferrite-sphere problems currently under investigation. Early in the study, it became apparent that the problem, although solvable in theory, was quite complex. The results expected as an extension of the sphere and cylinder problems seem desirable. However, great urgency of other parts of the project has deferred work in this area. Accordingly, only the first step of the solution was carried out and the method of solution indicated. But work will continue on the related problem of the radiation properties of a constant cur-

rent antenna embedded in a ferrite prolate spheroid.

Assume an incident plane wave propagating in the negative z direction. The electric vector has a magnitude E_O and points in the positive y direction; the magnetic vector points in the positive x direction. The ferrite prolate spheroid is located at the origin. The orientation of the spheroid and the incident wave striking nose-on are shown in Figs. 10 and 11.

Expanding the incident plane wave in spheroidal vector wave functions[2]

$$\underline{E}_i = \overline{a}_y E_O e^{j(kz-\omega t)} = \frac{-jE_O e^{-j\omega t}}{k} \sum_{\ell=0}^{\infty} A_{o\ell} \underline{x}_{\substack{M\\-o\ell}}^{(1)}$$

$$\underline{H}_i = \overline{a}_x \frac{\omega}{\mu k} E_O e^{j(kz-\omega t)} = \frac{\omega E_O e^{-j\omega t}}{\mu k^2} \sum_{\ell=0}^{\infty} A_{o\ell} \underline{x}_{\substack{N\\-o\ell}}^{(1)} \tag{36}$$

where

$$A_{o\ell} = \frac{2(j)^{\ell}}{\underline{N}_{o\ell}} \sum_{n=0,1}^{\infty'} (d_n^{o\ell})$$

$$\underline{N}_{o\ell} = \sum_{n=0,1}^{\infty'} \frac{2}{2(n+1)} (d_n^{o\ell})^2 \tag{37}$$

The prime on the summation indicates that the summation is to be over even values of n if ℓ is even, and over odd values of n if ℓ is odd. The symbols $d_n^{m\ell}$ are numerical coefficients tabulated by Stratton, Morse, Chu, and Hutner.[3] The expressions for the incident wave have the property that they are finite at all points in space.

2.3.1 Scattered Field. —At least eight sets of vector functions are available, the individual terms of each set satisfying the vector Helmholtz equation and having zero divergence.[2]

PROLATE SPHEROID
CHARACTERISTICS:
μ, ϵ
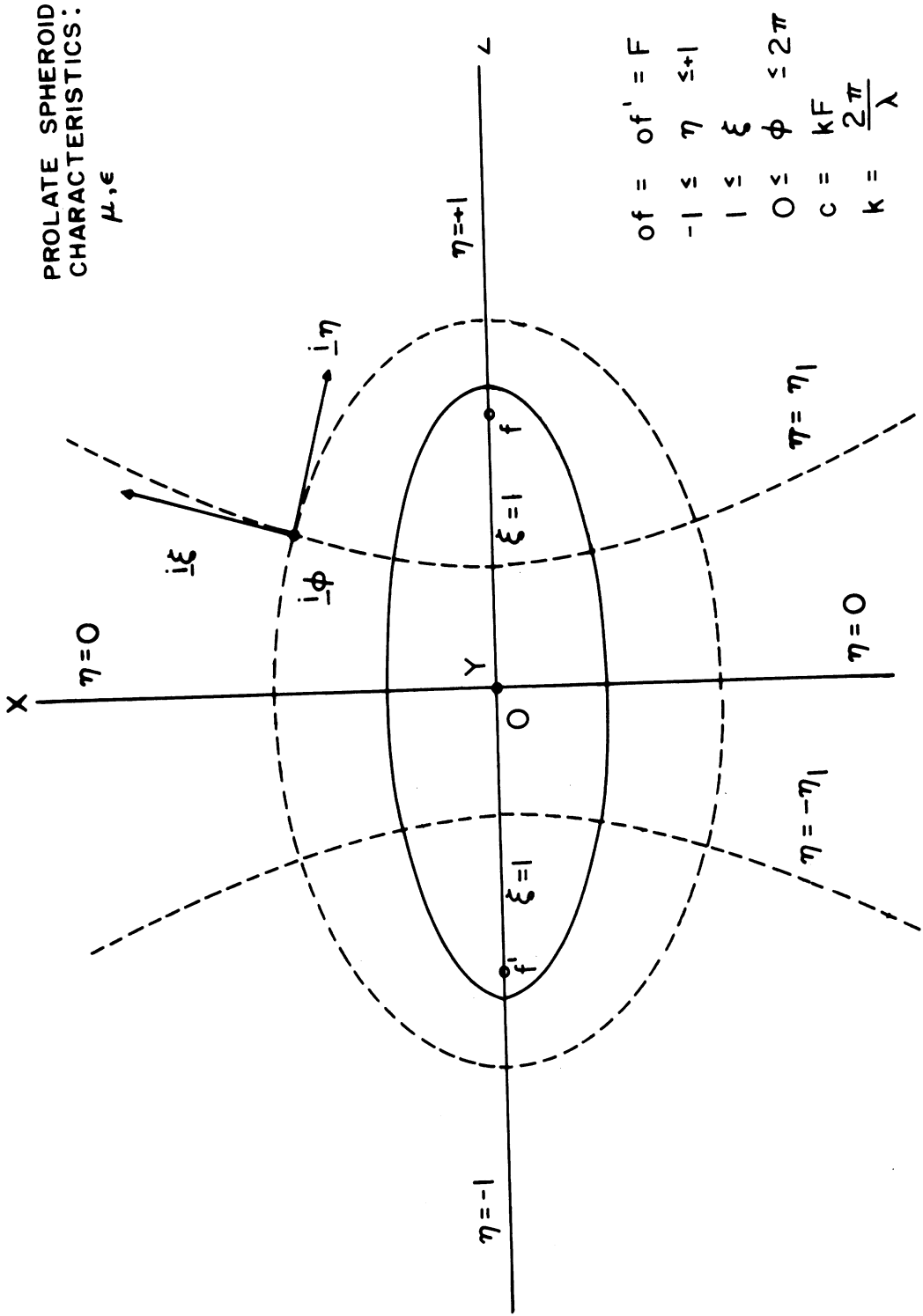
$of = of' = F$
$-1 \leqslant \eta \leqslant +1$
$1 \leqslant \xi$
$0 \leqslant \phi \leqslant 2\pi$
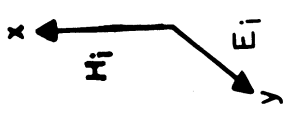$c = kF$
$k = \dfrac{2\pi}{\lambda}$
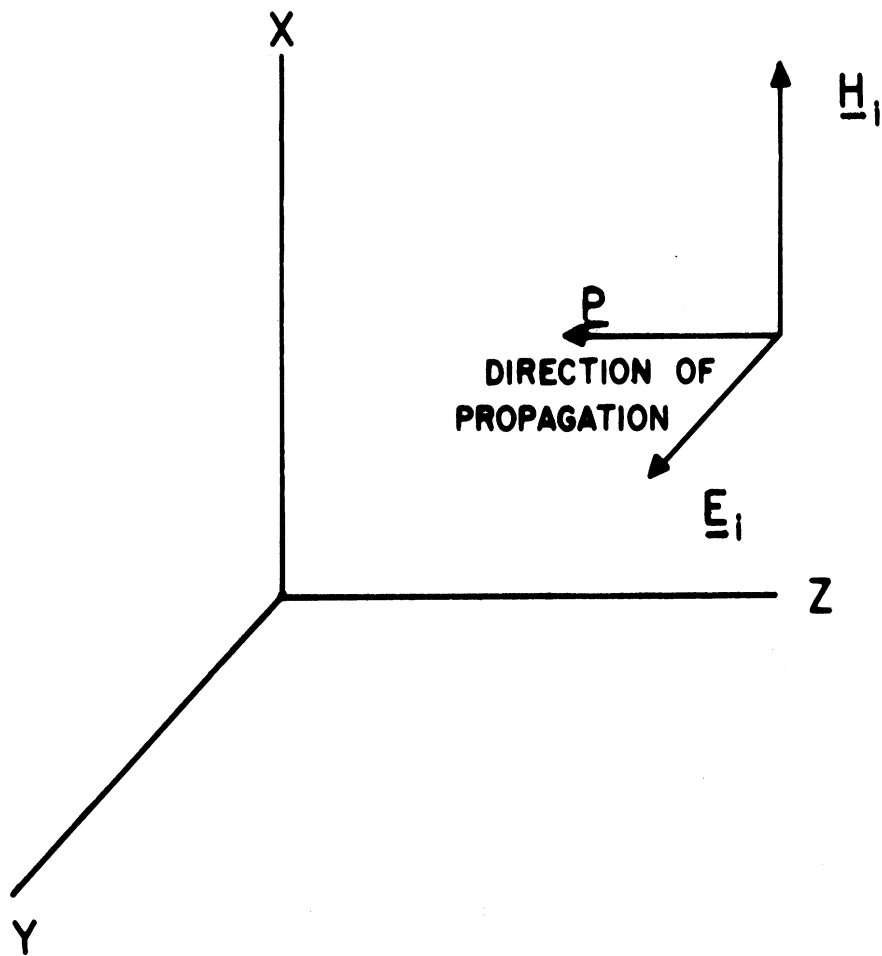
Fig. 10. Prolate spheroidal coordinates.

34

Fig. 11. Incident electromagnetic wave.

In choosing two of the eight sets of vector functions to represent the scattered wave, it is highly desirable to choose functions of each of the three components of which vary with ϕ in the same way as do the corresponding components of the incident wave. The vector functions which have the proper variation with ϕ are: ${}^{x}\underline{M}_{O\ell}^{(i)}$, ${}^{z}\underline{M}_{O\ell}^{(i)}$, ${}^{y}\underline{N}_{O\ell}^{(i)}$, ${}^{r}\underline{M}_{1\ell}^{(i)}$, and ${}^{r}\underline{N}_{1\ell}^{(i)}$. Of these ${}^{x}\underline{M}_{1\ell}^{(4)}$, ${}^{z}\underline{M}_{1\ell}^{(4)}$ were chosen for reasons of simplicity. However, the order (4) was chosen since $\underline{M}^{(4)}$ tends to $\frac{1}{r}\,e^{-j(\frac{2\pi r}{\lambda}\,-\,\text{const.})}$ as ξ tends to ∞, as is the case for the scattered wave. Now the expressions for the scattered wave are:

$$\underline{E}_{s} = \frac{-jE_{0}e^{-j\omega t}}{k}\sum_{\ell=0}^{\infty}\left[\alpha_{O\ell}^{s}\,{}^{x}\underline{M}_{O\ell}^{(4)} + \beta_{1\ell}^{s}\,{}^{z}\underline{M}_{1\ell}^{(4)}\right]$$

$$\underline{H}_{s} = \frac{\omega E_{0}e^{-j\omega t}}{\mu k^{2}}\sum_{\ell=0}^{\infty}\left[\alpha_{O\ell}^{s}\,{}^{x}\underline{N}_{O\ell}^{(4)} + \beta_{1\ell}^{s}\,{}^{z}\underline{N}_{1\ell}^{(4)}\right] \tag{38}$$

where $\alpha_{O\ell}^{s}$, $\beta_{1\ell}^{s}$ are unknown coefficients to be determined from the boundary conditions. The expressions for $\underline{M}$, $\underline{N}$ are given in Ref. 2.

The expressions for the transmitted field are:

$$\underline{E}_{t} = \frac{-jE_{0}e^{-j\omega t}}{k_{1}}\sum_{\ell=0}^{\infty}\left[\alpha_{O\ell}^{t}\,{}^{x}\underline{M}_{O\ell}^{(1)} + \beta_{1\ell}^{t}\,{}^{z}\underline{M}_{1\ell}^{(1)}\right]$$

$$\underline{H}_{t} = \frac{\omega E_{0}e^{-j\omega t}}{\mu_{1}k_{1}^{2}}\sum_{\ell=0}^{\infty}\left[\alpha_{O\ell}^{t}\,{}^{x}\underline{N}_{O\ell} + \beta_{1\ell}^{t}\,{}^{z}\underline{N}_{1\ell}\right] \tag{39}$$

where ${}^{x}\underline{M}_{O\ell}^{(1)}$, ${}^{z}\underline{M}_{1\ell}^{(1)}$ were chosen since they are regular (no singularity) along the line $\xi = 1$ (which is the degenerate spheroid), and since each of the components varies with ϕ in the same way as do the corresponding components of the incident wave.

2.3.2 Boundary Conditions.—

$$\underline{i}_\xi \times (\underline{E}_i + \underline{E}_s) = \underline{i}_\xi \times \underline{E}_t$$
$$\underline{i}_\xi \times (\underline{H}_i + \underline{H}_s) = \underline{i}_\xi \times \underline{H}_t \qquad \text{at } \xi = \xi_0 \qquad (40)$$

This results in four equations in the four unknowns $\alpha_{0\ell}^t$, $\alpha_{0\ell}^s$, $\beta_{1\ell}^t$, and $\beta_{1\ell}^s$.

These equations are:

$$\sum_{\ell=0}^{\infty} \left[\frac{k_1}{k} \beta_{1\ell}^s B_{L\ell} - \beta_{1\ell}^t C_{L\ell} + \alpha_{0\ell}^t D_{L\ell} - \frac{k_1}{k} E_{0\ell} \alpha_{L\ell}^s \right] = \frac{k_1}{k} \sum_{\ell=0}^{\infty} F_{0\ell}$$

$$\sum_{\ell=0}^{\infty} \left[-\frac{k_1}{k} \beta_{1\ell}^s G_{L\ell} + \beta_{1\ell}^t H_{L\ell} - \alpha_{0\ell}^t I_{L\ell} + \frac{k_1}{k} \alpha_{0\ell}^s J_{L\ell} \right] = -\frac{k_1}{k} \sum_{\ell=0}^{\infty} K_{L\ell}$$

$$\sum_{\ell=0}^{\infty} \left[\frac{\beta_{1\ell}^s}{\mu k^3} L_{L\ell} - \frac{\beta_{1\ell}^t}{\mu_1 k_1^3} M_{1\ell} + \frac{\alpha_{0\ell}^t}{\mu_1 k_1^3} N_{L\ell} - \frac{\alpha_{0\ell}^s}{\mu k^3} O_{L\ell} \right] = \frac{1}{\mu k^3} \sum_{\ell=0}^{\infty} P_{L\ell}$$

$$\sum_{\ell=0}^{\infty} \left[-\frac{\beta_{1\ell}^s}{\mu k^3} Q_{L\ell} + \frac{\beta_{1\ell}^t}{\mu_1 k_1^3} T_{L\ell} - \frac{\alpha_{0\ell}^t}{\mu_1 k_1^3} U_{L\ell} + \frac{\alpha_{0\ell}^s}{\mu k^3} V_{L\ell} \right] = -\frac{1}{k^3} \sum_{\ell=0}^{\infty} W_{L\ell} \qquad (41)$$

which are four infinite simultaneous equations. However, the constants $B_{L\ell}$, $C_{L\ell}, \ldots W_{L\ell}$ are not simple expressions. Each one of these constants is an infinite series containing very complicated integrals.

These constants are:²

$$B_{L\ell} = R_{1\ell}^{(4)}(\xi_o) \int_{-1}^{1} Si_\ell^{(1)}(\eta) So_L^{(1)}(\eta)\,\eta(1-\eta^2)^{-\frac{1}{2}} d\eta$$

$$C_{L\ell} = R_{1\ell}^{(1)}(\xi_o) \int_{-1}^{1} Si_\ell^{(1)}(\eta) So_L^{(1)}(\eta)\,\eta(1-\eta^2)^{-\frac{1}{2}} d\eta$$

$$D_{L\ell} = R_{o\ell}'^{(1)}(\xi_o)(\xi_o^2-1)^{\frac{1}{2}} \int_{-1}^{1} So_\ell^{(1)}(\eta) So_L^{(1)}(\eta)\,d\eta$$

$$E_{L\ell} = R_{o\ell}'^{(4)}(\xi_o)(\xi_o^2-1)^{\frac{1}{2}} \int_{-1}^{1} So_\ell^{(1)}(\eta) So_L^{(1)}(\eta)\,d\eta$$

$$F_{L\ell} = A_{o\ell} R_{o\ell}'^{(1)}(\xi_o)(\xi_o^2-1)^{\frac{1}{2}} \int_{-1}^{1} So_\ell^{(1)}(\eta) So_L^{(1)}(\eta)\,d\eta = A_{o\ell} D_{o\ell}$$

$$G_{L\ell} = \xi_o(\xi_o^2-1)^{\frac{1}{2}} R_{1\ell}^{(4)}(\xi_o) \int_{-1}^{1} Si_\ell^{(1)}(\eta) So_L^{(1)}(\eta)(1-\eta^2)^{\frac{1}{2}} d\eta - (\xi_o^2-1)^{\frac{1}{2}} R_{1\ell}^{(4)}(\xi_o) \int_{-1}^{1} Si_\ell^{(1)}(\eta) So_L^{(1)}(\eta)\,\eta(1-\eta^2)^{\frac{1}{2}} d\eta$$

$$H_{L\ell} = \xi_o(\xi_o^2-1)^{\frac{1}{2}} R_{1\ell}^{(1)}(\xi_o) \int_{-1}^{1} Si_\ell^{(1)}(\eta) So_L^{(1)}(\eta)(1-\eta^2)^{\frac{1}{2}} d\eta - (\xi_o^2-1)^{\frac{1}{2}} R_{1\ell}^{(1)}(\xi_o) \int_{-1}^{1} Si_\ell^{(1)}(\eta) So_L^{(1)}(\eta)\,\eta(1-\eta^2)^{\frac{1}{2}} d\eta$$

$$I_{L\ell} = (\xi_o^2-1) R_{o\ell}'^{(1)}(\xi_o) \int_{-1}^{1} So_\ell^{(1)}(\eta) So_L^{(1)}(\eta)\,\eta\,d\eta + \xi_o R_{o\ell}^{(1)}(\xi_o) \int_{-1}^{1} So_\ell^{(1)}(\eta) So_L^{(1)}(\eta)(1-\eta^2)\,d\eta$$

$$J_{L\ell} = (\xi_o^2-1) R_{o\ell}'^{(4)}(\xi_o) \int_{-1}^{1} So_\ell^{(1)}(\eta) So_L^{(1)}(\eta)\,\eta\,d\eta + \xi_o R_{o\ell}^{(4)}(\xi_o) \int_{-1}^{1} So_\ell^{(1)}(\eta) So_L^{(1)}(\eta)(1-\eta^2)\,d\eta$$

$$K_{L\ell} = (\xi_o^2-1) R_{o\ell}'^{(1)}(\xi_o) A_{o\ell} \int_{-1}^{1} So_\ell^{(1)}(\eta) So_L^{(1)}(\eta)\,\eta\,d\eta + \xi_o R_{o\ell}^{(1)}(\xi_o) A_{o\ell} \int_{-1}^{1} So_\ell'^{(1)}(\eta) So_L^{(1)}(\eta)(1-\eta^2)\,d\eta$$

$$(42)$$

38

or

$$K_{L\ell} = A_{L\ell}\,{}^{1}L_\ell$$

$$L_{L\ell} = \int_{-1}^{1} Si_\ell^{(1)}(\eta)\,So_L^{(1)}(\eta)\,\eta(1-\eta^2)^{\frac12}\frac{\partial}{\partial\xi_o}\left[\frac{\xi_o^2-1}{\xi_o^2-\eta^2}Ri_\ell^{(4)}(\xi_o)\right]d\eta$$
$$+\,\xi_o(\xi_o^2-1)^{-1}Ri_\ell^{(4)}(\xi_o)\int_{-1}^{1} Si_\ell^{(1)}(\eta)\,So_L^{(1)}(\eta)(1-\eta^2)^{-\frac12}\,d\eta$$

$$M_{L\ell} = \int_{-1}^{1} Si_\ell^{(1)}(\eta)\,So_L^{(1)}(\eta)\,\eta(1-\eta^2)^{\frac12}\frac{\partial}{\partial\xi_o}\left[\frac{(\xi_o^2-1)Ri_\ell^{(1)}(\xi_o)}{\xi_o^2-\eta^2}\right]d\eta$$
$$+\,\xi_o(\xi_o^2-1)^{-1}Ri_\ell^{(1)}(\xi_o)\int_{-1}^{1} Si_\ell^{(1)}(\eta)\,So_L^{(1)}(\eta)(1-\eta^2)^{-\frac12}\,d\eta$$

$$N_{L\ell} = \int_{-1}^{1} So_\ell^{(1)}(\eta)\,So_L^{(1)}(\eta)\,\eta(1-\eta^2)\frac{\partial}{\partial\xi_o}\left[\frac{(\xi_o^2-1)^{\frac32}}{(\xi_o^2-\eta^2)}Ro_\ell'^{(1)}(\xi_o)\right]d\eta + \frac{Ro_\ell^{(1)}(\xi_o)}{(\xi_o^2-1)^{\frac12}}\int_{-1}^{1} So_\ell'^{(1)}(\eta)\,So_L^{(1)}(\eta)\,d\eta - \int_{-1}^{1} Si_\ell'^{(1)}(\eta)\,So_L^{(1)}(\eta)\,d\eta + \int_{-1}^{1} So_\ell^{(1)}(\eta)\,So_L^{(1)}(\eta)(1-\eta^2)\frac{\partial}{\partial\xi_o}\left[\frac{\xi_o(\xi_o^2-1)^{\frac12}}{(\xi_o^2-\eta^2)}Ro_\ell^{(1)}(\xi_o)\right]d\eta$$

$$O_{L\ell} = \int_{-1}^{1} So_\ell^{(1)}(\eta)\,So_L^{(1)}(\eta)\,\eta(1-\eta^2)\frac{\partial}{\partial\xi_o}\left[\frac{(\xi_o^2-1)^{\frac32}}{(\xi_o^2-\eta^2)}Ro_\ell'^{(4)}(\xi_o)\right]d\eta + \frac{Ro_\ell^{(4)}(\xi_o)}{(\xi_o^2-1)^{\frac12}}\int_{-1}^{1} So_\ell'^{(1)}(\eta)\,So_L^{(1)}(\eta)\,d\eta - \int_{-1}^{1} So_\ell^{(1)}(\eta)\,So_L^{(1)}(\eta)(1-\eta^2)\frac{\partial}{\partial\xi_o}\left[\frac{\xi_o(\xi_o^2-1)^{\frac12}}{(\xi_o^2-\eta^2)}Ro_\ell^{(4)}(\xi_o)\right]d\eta$$

$$P_{L\ell} = -\,A_{L\ell}N_{L\ell}$$

$$Q_{L\ell} = \frac{\xi_o Ri_\ell^{(4)}(\xi_o)}{\xi_o^2-1}\int_{-1}^{1} Si_\ell^{(1)}(\eta)\,So_L^{(1)}(\eta)\,d\eta + Ri_\ell^{(4)}(\xi_o)\int_{-1}^{1} Si_\ell'^{(1)}(\eta)\,So_L^{(1)}(\eta)\frac{\eta}{1-\eta^2}\,d\eta$$

$$T_{L\ell} = \frac{\xi_o Ri_\ell^{(1)}(\xi_o)}{\xi_o^2-1}\int_{-1}^{1} Si_\ell^{(1)}(\eta)\,So_L^{(1)}(\eta)\,d\eta + Ri_\ell^{(1)}(\xi_o)\int_{-1}^{1} Si_\ell'^{(1)}(\eta)\,So_L^{(1)}(\eta)\frac{\eta}{1-\eta^2}\,d\eta$$

$$U_{L\ell} = \frac{Ro_\ell^{(1)}(\xi_o)}{(\xi_o^2-1)^{\frac12}}\int_{-1}^{1} So_L^{(1)}\frac{d}{d\eta}\left[(1-\eta^2)^{\frac12}So_\ell'^{(1)}(\eta)\right]d\eta + \frac{d}{d\xi_o}\left[(\xi_o^2-1)^{\frac12}Ri_\ell^{(1)}(\xi_o)\right]\int_{-1}^{1} So_L^{(1)}(\eta)\,So_\ell^{(1)}(\eta)(1-\eta^2)^{-\frac12}\,d\eta$$

$$V_{L\ell} = \frac{Ro_\ell^{(4)}(\xi_o)}{(\xi_o^2-1)^{\frac12}}\int_{-1}^{1} So_L^{(1)}\frac{d}{d\eta}\left[(1-\eta^2)^{\frac12}So_\ell'^{(1)}(\eta)\right]d\eta + \frac{d}{d\xi_o}\left[(\xi_o^2-1)^{\frac12}R_\ell'^{(4)}(\xi_o)\right]\int_{-1}^{1} Si_\ell'^{(1)}(\eta)\,So_L^{(1)}(\eta)(1-\eta^2)^{\frac12}\,d\eta$$

$$W_{L\ell} = A_{L\ell}U_{L\ell}$$

39

In Eq. (41) both ℓ, L go from zero to infinity. The prime on R and S

indicates differentiation with respect to the argument.

The procedure used to evaluate the above integrals is to express $S_{m\ell}^{(1)}(\eta)$

and its derivatives in terms of $P_{m+n}^m(\eta)$ and its derivatives.[2]

The difficulty in solving this problem comes from the fact that the vec-

tor wave functions in spheroidal coordinates are not orthogonal as in spherical

and cylindrical coordinates. In spherical or cylindrical coordinates, the

vector wave functions, under certain conditions, satisfy

$$
\left.
\begin{array}{l}
\iint\limits_{S} \bar{V}_n \cdot \bar{V}_m ds = 0 \\[4mm]
\iint\limits_{S} \bar{U}_n \cdot \bar{U}_m ds = 0
\end{array}
\right\} \quad n \neq m \tag{43}
$$

and

$$
\iint\limits_{S} \bar{V}_n \cdot \bar{U}_n ds = 0
$$

This orthogonality makes it possible in the sphere and cylinder to get four

equations only. Unfortunately, these relations do not hold in the spheroidal

case, but they do for the scalar wave functions from which the vector wave

functions are derived.[5]

The four infinite simultaneous equations can be solved by taking a

finite number of terms (for example, two terms), and then solving the result-

ing equations

2.4 RADIATION FROM A MATERIAL-FILLED RECTANGULAR-WAVEGUIDE H-PLANE SECTORAL HORN

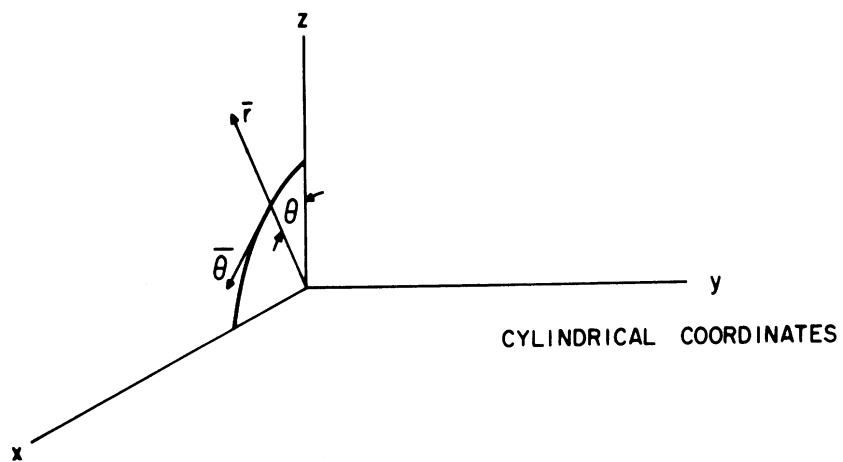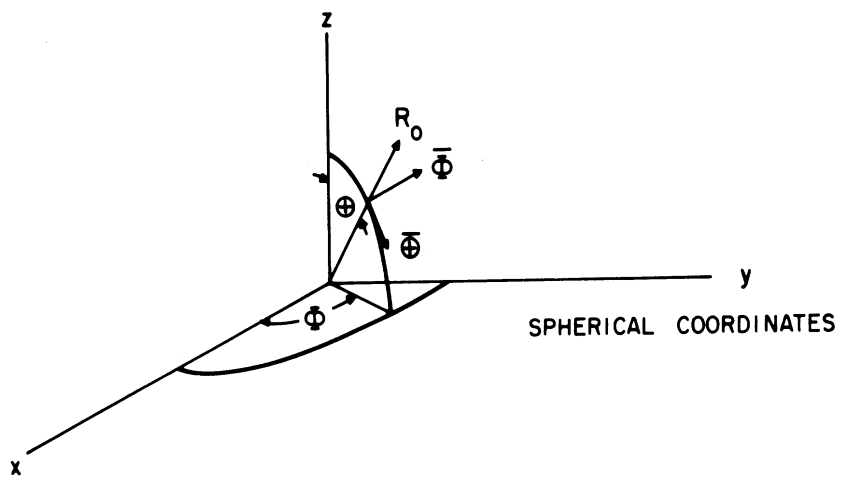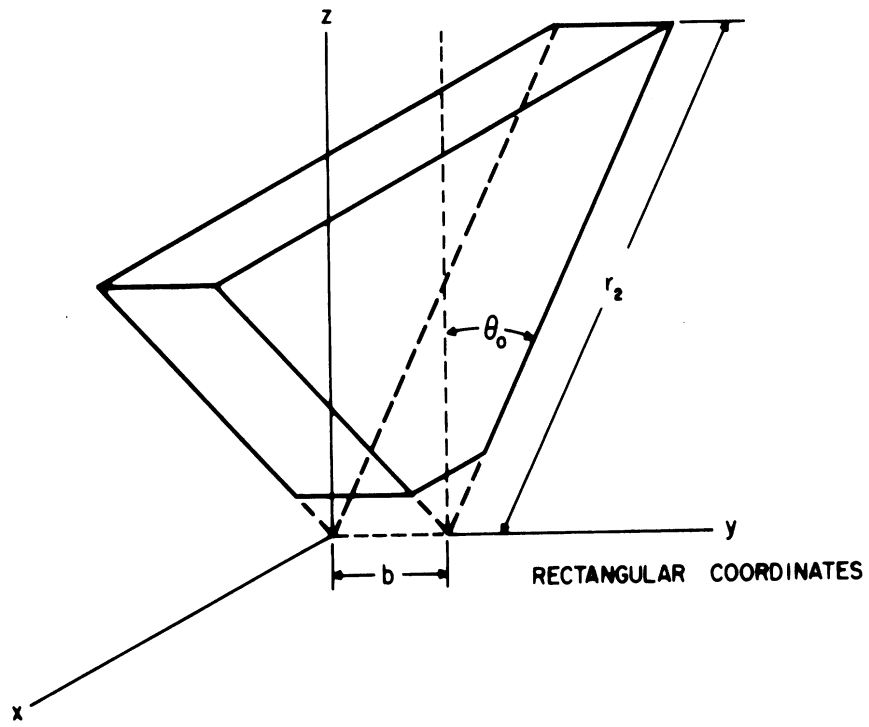The H-plane sectoral horn, shown in Fig 12, has been evaluated the-

Fig. 12. Coordinate systems used for H-plane horn.

oretically. The horn and waveguide are assumed to be filled with a material

of relative permeability μ_r and relative permittivity ϵ_r. The derivation for

the radiated fields is similar to that done by Silver[6] for an air-filled

horn. Huygens' principle is used and the source replaced by the fields in

the aperture. To simplify the solution, the current distribution over the

exterior surface of the waveguide is neglected. It is also assumed that only

the TE_0 mode exists in the rectangular waveguide feed and that only one mode

propagates in the sectoral guide due to the dimensions of the horn throat

and the excitation.

Referring to Fig. 12, the only fields present in the horn are E_y, H_r, and

H_θ, because these fields match with the TE_{10} components in the rectangular

waveguide feed.

To determine the space dependence of the fields in the horn, Maxwell's

equations are solved in cylindrical coordinates. By applying the boundary con-

ditions and solving, the following fields are obtained.

$$E_y = \cos p\theta \left[H_p^{(2)}(k_1 r) + \alpha H_p^{(1)}(k_1 r) \right]$$

$$H_r = \frac{p \sin p\theta}{j\omega\mu r} \left[H_p^{(2)}(k_1 r) + \alpha H_p^{(1)}(k_1 r) \right] \tag{44}$$

$$H_\theta = \frac{k_1 \cos p\theta}{j\omega\mu} \left[H_p'^{(2)}(k_1 r) + \alpha H_p'^{(1)}(k_1 r) \right]$$

where:

$H_p^{(2)}(k_1 r)$ = the Hankel function of order two, representing
an outward traveling wave.

$H_p^{(1)}(k_1 r)$ = the Hankel function of order one, representing
an inward traveling wave.

$$P = \frac{\pi}{2\theta_O}, \text{ usually not an integer}$$

$$\theta_O = \text{the flare angle}$$

$$\alpha = \text{reflection coefficient from the horn to free space.}$$

Primes represent derivatives with respect to $k r$.

$$k_1 = \omega\sqrt{\mu\epsilon}$$

$$\mu = \text{permeability of the material inside the horn}$$

$$\epsilon = \text{permittivity of the material inside the horn}$$

$$\omega = \text{frequency of operation.}$$

To determine the radiated fields, the aperture diffraction method is used. The sources are replaced by the fields at the aperture of the horn and the far-field pattern is derived from this distribution.

As shown by Silver (Ref. 6, p. 161), the radiated far field is given by:

$$E_p = -\frac{jk}{4\pi r} e^{-jkR} \bar{R}_O \times \int_{aperture} \left[\bar{n} \times \bar{E} - \sqrt{\frac{\mu_O}{\epsilon_O}} \bar{R}_O \times (\bar{n} \times \bar{H}) \right] e^{jk\bar{\rho} \cdot \bar{R}_O} ds \qquad (45)$$

where:

$$\bar{R}_O = \text{a unit vector from the origin to the field point}$$

$$\bar{n} = \text{outward normal to the aperture, in this case the cylindrical } \bar{r} \text{ unit vector.}$$

$$\bar{E}, \bar{H} = \text{the fields at the aperture of the horn, } r = r_2$$

$$k = \omega\sqrt{\mu_O\epsilon_O} = \text{free space propagation factor}$$

$$\mu_O, \epsilon_O = \text{permeability and permittivity of free space}$$

$$\bar{\rho} = \text{vector from the origin to the element ds of the aperture area}$$

$$R = \text{spherical coordinate of the field point.}$$

Carrying out the calculations, the following fields are found:

(a) for the yZ-plane, or E-plane, $\phi = 90°$

$$E_\theta = i_\theta j \frac{kV_2}{4\pi R} e^{-jkR} \int_0^b \int_{-\theta_0}^{\theta_0} e^{jk(V_2 \cos\theta\cos\theta + y\sin\theta)}$$

$$\left[\cos\theta E_y - \sqrt{\frac{\mu_0}{\epsilon_0}} \cos\theta H_\theta\right] d\theta dy \tag{46}$$

(b) for the xZ-plane, or H-plane, $\phi = 0°$

$$E_\phi = i_\phi \frac{jkr_2 e^{-jkR}}{4\pi R} \int_0^b \int_{-\theta_0}^{\theta_0} e^{jkr_2(\sin\theta\sin\theta + \cos\theta\cos\theta)}$$

$$\left[\cos(\theta-\theta) E_y - \sqrt{\frac{\mu_0}{\epsilon_0}} H_\theta\right] d\theta dy \tag{47}$$

where:

i_θ = unit vector in θ direction

i_ϕ = unit vector in ϕ direction

E_y = from Eq. (1) with $r = r_2$

H_θ = from Eq. (3) with $r = r_2$.

Then, substituting Eqs. (1) and (3) into Eqs. (5) and (6), the far fields are found to be:

(a) E-plane, $\phi = 90°$

$$E_\theta = i_\theta j \frac{kr_2 e^{-jkR}}{4\pi R} \int_0^b e^{jk\sin\theta y} dy \int_{-\theta_0}^{\theta_0} e^{jkr_2(\cos\theta\cos\theta)}$$

$$\left\{\cos\theta\cos\rho\theta \left[H_\rho^{(2)}(k_1 V_2) + \alpha H_\rho^{(1)}(k_1 V_2)\right] - \sqrt{\frac{\mu_0}{\epsilon_0}} \cos\theta \frac{k_1}{j\omega\mu}\right.$$

$$\left.\cos\rho\theta \left[H_\rho'^{(2)}(k_1 V_2) + \alpha H_\rho'^{(1)}(k_0 r_2)\right]\right\} d\theta \tag{48}$$

44

(b) H-plane, $\phi = 0°$

$$E_\phi = j \frac{kV_2 e^{-jkR}}{4\pi R} \int_0^b \int_{-\theta_0}^{\theta_0} e^{jkr_2(\sin\theta\sin\Theta + \cos\theta\cos\Theta)}$$

$$\left\{ \cos(\theta-\Theta) \cos \rho\Theta \left[H_\rho'^{(2)}(k_1 V_2) + \alpha H_\rho'^{(1)}(k_1 r_2) \right] - j\sqrt{\frac{\mu_0}{\epsilon_0}} \frac{k_1}{j\omega\mu} \right.$$

$$\left. \cos \rho\Theta \left[H_\rho'^{(2)}(k_1 V_2) + \alpha H_\rho'^{(1)}(k_1 V_2) \right] \right\} \, d\Theta dy \qquad (49)$$

The integrals in Eqs. (7) and (8) can be evaluated easily using numerical integration on a computer. A program has been written, and results of the calculations will be given in the next Quarterly.

2.5 RADIATION FROM HORNS FLARED IN TWO DIMENSIONS AND FILLED WITH FERRITE MATERIAL

The procedure followed is to solve the vector wave equation in spherical coordinates such that the boundary conditions are satisfied on the surface of the horn. Then, assuming that the horn supports only one mode, which corresponds to the TE_{10} mode of the exciting rectangular guide, the fields at the aperture are evaluated and used in the modified Kirchoff formula to obtain the radiation field.

The horn is defined by the cones $\Theta = \Theta_1$, $\Theta = \pi - \Theta_1$, the planes $\phi = 0$, $\phi = \phi_1$ and the spheres $r = r_1$ $r = r_2$ as shown in Fig. 13.

The vector wave equation $\nabla^2\overline{C} + k^2\overline{C} = 0$ has two solutions $\overline{M}$, $\overline{N}$ which have zero divergence. These two solutions could be obtained from the solution of the scalar wave equation $\nabla^2\psi + k^2\psi = 0$. The general solution of the scalar wave equation in spherical coordinates is
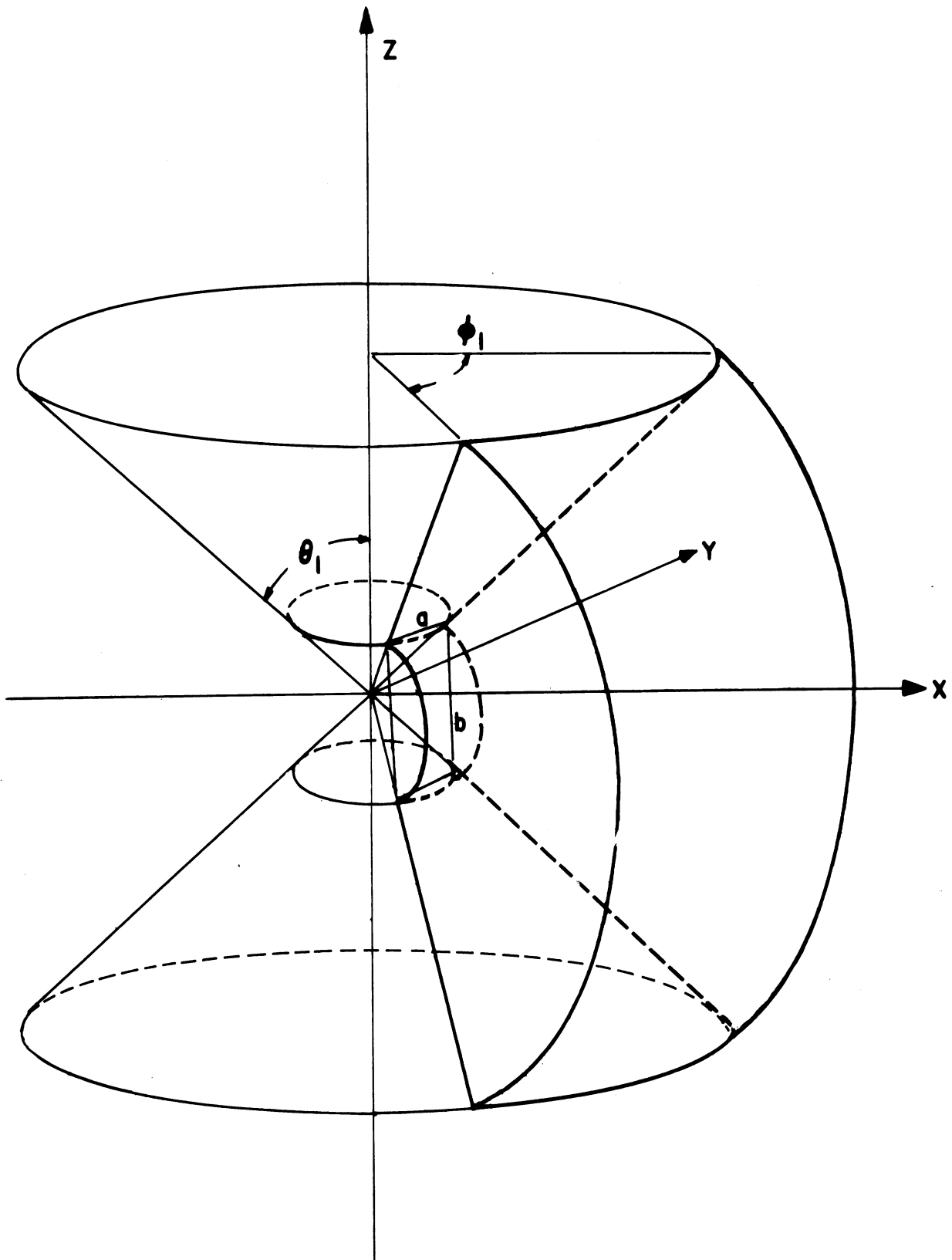
Fig. 13. Double-taper ferrite-filled horn.

$$\psi_{mn} = (A_m \cos m\phi + B_m \sin m\phi) \left[C_{nm}P_n^m(\cos \theta) + D_{nm}P_n^m(-\cos \theta) \right] \left[E_n h_n^{(1)}(kr) \right.$$

$$\left. + F_n h_n^{(2)}(kr) \right] \tag{50}$$

$h_n^{(1)}$, $h_n^{(2)}$ have been taken to represent traveling and reflected waves. n,m are not integers because the region $\theta = 0$, $\theta = \pi$ is excluded and there are boundaries in the ϕ-direction.

$$M_1 = 0$$

$$M_2 = \frac{1}{\sin \theta} \frac{\partial \psi}{\partial \phi}$$

$$= \frac{1}{\sin \theta} (- mA_m \sin m\phi + mB_m \cos m\phi) \left[C_{nm}P_n^m(\cos \theta) + D_{nm}P_n^m(-\cos \theta) \right]$$

$$\left[E_n h_n^{(1)}(kr) + F_n h_n^{(2)}(kr) \right]$$

$$M_3 = - \frac{\partial \psi}{\partial \theta}$$

$$= - (A_m \cos m\phi + B_m \sin m\phi) \left[C_{nm} \frac{\partial P_n^m(\cos \theta)}{\partial \theta} + D_{nm} \frac{\partial P_n^m(\cos \theta)}{\partial \theta} \right]$$

$$\left[E_n h_n^{(1)}(kr) + F_n h_n^{(2)}(kr) \right] \tag{51}$$

$$N_1 = \frac{n(n+1)}{kr} \psi_{mn}$$

$$= \frac{n(n+1)}{kr} (A_m \cos m\phi + B_m \sin m\phi) \left[C_{nm}P_n^m(\cos \theta) + D_{nm}P_n^m(-\cos \theta) \right] \left[E_n h_n^{(1)}(kr) + F_n h_n^{(2)}(kr) \right]$$

$$N_2 = \frac{1}{kr} \frac{\partial^2(k\psi)}{\partial r \partial \theta}$$

$$= \frac{1}{kr} (A_m \cos m\phi + B_m \sin m\phi) \left[C_{nm} \frac{\partial P_n^m(\cos \theta)}{\partial \theta} + D_{nm} \frac{\partial P_n^m(-\cos \theta)}{\partial \theta} \right] \left\{ E_n \frac{\partial}{\partial r} \left[kh_n^{(1)}(kr) \right] \right.$$

$$\left. + F_n \frac{\partial}{\partial r} \left[rh_n^{(2)}(kr) \right] \right\}$$

$$N_3 = \frac{1}{kr \sin \theta} \frac{\partial^2 r\psi}{\partial r \partial \phi}$$

$$= \frac{1}{kr \sin \theta} (-mA_m \sin m\phi + mB_m \cos m\phi) \left[C_{nm}P_n^m(\cos \theta) + D_{nm}P_n^m(-\cos \theta) \right] \left\{ E_n \frac{\partial}{\partial r} \left[kh_n^{(1)}(kr) \right] \right.$$

$$\left. + F_n \frac{\partial}{\partial r} \left[rh_n^{(2)}(kr) \right] \right\} \tag{52}$$

$$\overline{E} = \sum_{n,m} (\overline{M}_n + b_n \overline{N}_n)$$

$$\overline{H} = \frac{k}{j\omega\mu} \sum_{n,m} (\overline{N}_n + b_n \overline{M}_n) \tag{53}$$

Now the boundary conditions to be satisfied are:

$$E_1 = E_2 = 0 \quad \text{on} \quad \phi = 0, \; \phi = \phi_2$$

$$E_1 = E_3 = 0 \quad \text{on} \quad \theta = \theta_1, \; \theta = \pi-\theta_1 \qquad r_1 < r \leq r_2$$

where:

the subscripts 1, 2, 3 refer to r, θ and ϕ components, respectively.

$$E_1 = \sum_{n,m} b_n \frac{n(n+1)}{kr} (A_m \cos m\phi + B_m \sin m\phi) \left[C_{nm} P_n^m(\cos \theta) + D_{nm} P_n^m(-\cos \theta) \right.$$

$$\left[E_n h_n^{(1)}(kr) + F_n h_n^{(2)}(kr) \right]$$

$$= 0 \quad \text{at} \quad \phi = 0, \quad \phi = \phi_2.$$

The only way to satisfy this condition and the others is to take $b_n = 0$.

Therefore

$$E_1 \equiv 0$$

From the condition on E_2 we get

$$B_m = 0, \quad m\phi_1 = \ell\pi, \quad \ell = 1, 2, 3, \ldots \tag{54}$$

From the conditions on E_3 we get

$$C_{nm} \frac{\partial P_n^m(\cos \theta_1)}{\partial \theta_1} + D_{nm} \frac{\partial P_n^m(-\cos \theta_1)}{\partial \theta_1} = 0$$

$$C_{nm} \frac{\partial P_n^m(-\cos \theta_1)}{\partial \theta_1} + D_{nm} \frac{\partial P_n^m(\cos \theta_1)}{\partial \theta_1} = 0$$

Therefore

$$\left[\frac{\partial P_n^m(\cos\,\Theta_1)}{\partial\Theta_1}\right]^2 = \left[\frac{\partial P_n^m(-\cos\,\Theta_1)}{\partial\Theta_1}\right]^2$$

Therefore

$$\frac{\partial P_n^m(\cos\,\Theta_1)}{\partial\Theta_1} = \pm\frac{\partial P_n^m(-\cos\,\Theta_1)}{\partial\Theta_1} \tag{55}$$

the characteristic Eq. (55) determines n. If ℓ is taken to be 1, then the

field components will be

$$E_r = 0$$

$$E_\Theta = -\frac{E_0\pi}{\phi_1\sin\,\Theta}\,\sin\,\frac{\pi\phi}{\phi_1}\left[\frac{\partial P_n^m(\cos\,\Theta_1)}{\partial\Theta_1}P_n^m(-\cos\,\Theta) - \frac{\partial P_n^m(-\cos\,\Theta_1)}{\partial\Theta_1}P_n^m(\cos\,\Theta)\right]$$

$$\left[h_n^{(2)}(kr) + \gamma_n h_n^{(1)}(kr)\right]$$

$$E_\phi = E_0\cos\,\frac{\pi\phi}{\phi_1}\left[\frac{\partial P_n^m(\cos\,\Theta_1)}{\partial\Theta_1}\frac{\partial P_n^m(-\cos\,\Theta)}{\partial\Theta} - \frac{\partial P_n^m(-\cos\,\Theta_1)}{\partial\Theta_1}\frac{\partial P_n^m(\cos\,\Theta)}{\partial\Theta}\right]$$

$$\left[h_n^{(2)}(kr) + \gamma_n h_n^{(1)}(kr)\right]$$

$$H_r = \frac{E_0 kn(n+1)}{j\omega y}\,\cos\,\frac{\pi d}{\phi_1}\left[\frac{\partial P_n^m(\cos\,\Theta_1)}{\partial\Theta_1}P_n^m(-\cos\,\Theta) - \frac{\partial P_n^m(-\cos\,\Theta_1)}{\partial\Theta_1}P_n^m(\cos\,\Theta)\right]$$

$$\left[\frac{h_n^{(2)}(kr)}{kr} + \gamma_n\frac{h_n^{(1)}(kr)}{kr}\right]$$

$$H_\Theta = \frac{E_0 k}{j\omega y}\,\cos\,\frac{\pi\phi}{\phi_1}\left[\frac{\partial P_n^m(\cos\,\Theta_1)}{\partial\Theta_1}\frac{\partial P_n^m(-\cos\,\Theta)}{\partial\Theta} - \frac{\partial P_n^m(-\cos\,\Theta_1)}{\partial\Theta_1}\frac{\partial P_n^m(\cos\,\Theta)}{\partial\Theta}\right]$$

$$\left\{\frac{1}{kr}\frac{\partial}{\partial r}\left[rh_n^{(2)}(kr)\right] + \frac{\gamma_n}{kr}\frac{\partial}{\partial r}\left[rh_n^{(1)}(kr)\right]\right\}$$

$$H_\phi = \frac{E_0 k\pi}{j\omega y\,\phi_1\sin\,\Theta}\,\sin\,\frac{\pi\phi}{\phi_1}\left[\frac{\partial P_n^m(\cos\,\Theta_1)}{\partial\Theta_1}P_n^m(-\cos\,\Theta) - \frac{\partial P_n^m(-\cos\,\Theta_1)}{\partial\Theta_1}P_n^m(\cos\,\Theta)\right]$$

$$\left\{\frac{1}{kr}\frac{\partial}{\partial r}\left[rh_n^{(2)}(kr)\right] + \frac{\gamma_n}{kr}\frac{\partial}{\partial r}\left[rh_n^{(1)}(kr)\right]\right\} \tag{56}$$

where:

$$m = \frac{\pi}{\phi_1}$$

      n   is given by the characteristic Eq. (55).

If ϕ_1 is taken to be $30°$ then m = 6.

Then:

$$P_\gamma^m(x) = \frac{(-)^m(\gamma+m)!}{2^m(2-m)!\,m!} (x^2-1)^{m/2} F(m-\gamma,\; m+\gamma+1,\; m+1,\; \frac{1-x}{2}) \quad \text{(Ref. 7, p. 428)}$$

where:

      F is hypergeometric function.

Therefore

$$P_\gamma^m(\cos\theta_1) = \frac{(-)^m(\gamma+m)!\sin^m\theta_1}{2^m(\gamma-m)!\,m!} F(m-\gamma,\; m+\gamma+1,\; m+1,\; \frac{1-\cos\theta_1}{2})$$

$$F(m-\gamma,\; m+\gamma+1,\; m+1,\; \frac{1-\cos\theta_1}{2}) = F_t$$

$$= 1 + \frac{m!}{(m-\gamma-1)!(m+\gamma)!} \sum_{\ell=0}^{\infty} \frac{(m-\gamma+\ell)!(m+\gamma+1+\ell)!}{\ell!(m+1+\ell)!} \left(\frac{1-\cos\theta_1}{2}\right)^{\ell+1}$$

$$\frac{\partial P_\gamma^m(\cos\theta_1)}{\partial\theta} = \frac{(-)^m(\gamma+m)!}{2^m(\gamma-m)!\,m!} \left[\sin^m\theta_1 \frac{\partial F_1}{\partial\theta_1} + m\cos\theta_1 \sin^{m-1}\theta_1 F_t\right]$$

$$\frac{\partial F_1}{\partial\theta_1} = \frac{m!\sin\theta_1}{2(m-\gamma-1)!(m+\gamma)!} \sum_{\ell=0}^{\infty} \frac{(m-\gamma+\ell)!(m+\gamma+1+\ell)!}{\ell!(m+1+\ell)!} (\ell+1)\left(\frac{1-\cos\theta_1}{2}\right)^{\ell}$$

after getting the corresponding expression for F, substituting in Eq. (55) and

manipulating, we get:

$$\sum_{\ell=0}^{\infty} \frac{(m-\gamma+\ell)!(m+\gamma+1+\ell)!}{\ell!(m+1+\ell)!} \left\{ \frac{(\ell+1)\sin^2\theta_1}{2}\left[\left(\frac{1-\cos\theta_1}{2}\right)^{\ell}\right.\right. \quad (57)$$

$$\left.\left.\pm \left(\frac{1+\cos\theta_1}{2}\right)^{\ell}\right] + m\cos\theta_1\left(\frac{1-\cos\theta_1}{2}\right)^{\ell+1} \mp \left(\frac{1+\cos\theta_1}{2}\right)^{\ell+1}\right\} = 0$$

Before specific values for θ_1 are taken, the dimensions of the feeding guide should be considered. Assuming the rectangular guide supports only TE_{10} mode, the dimensions of the guide must be

$$a < \lambda < 2a, \quad 2b < \lambda$$

Therefore

$$b < a$$

$$a = 2r_1 \sin \theta_1 \sin \frac{\phi_1}{2}$$

$$b = 2r_1 \sin (\lambda - 2\theta_1)$$

Therefore

$$\sin(\pi - 2\theta_1) < \sin \theta_1 \sin \frac{\phi_1}{2}$$

i.e.,

$$\cos \theta_1 < \frac{1}{2} \sin \frac{\phi_1}{2} \tag{58}$$

for

$$\phi_1 = 30°$$

therefore

$$\cos \theta_1 < 0.1295$$

therefore

$$\phi_1 > 82.5°$$

therefore the angle of the cone is less than $15°$, and we notice from Eq. (58) that, as ϕ_1 increases, the minimum value of the angle of the horn in the θ-direction increases.

Equation (10) is solved approximately by taking the first ten terms, for example, instead of the infinite summation, calculating the value of the summation for different values of γ, $\gamma = 4.5, 5.5, 6.5, 7.5, 8.5, 9.5$, plotting

the summation vs. γ, and then taking the value of γ for which the summation

is zero. To evaluate negative factorials, the definitions $(-x)! = \dfrac{\pi}{(x-1)!\sin\pi x}$;

$(-\frac{1}{2})! = \sqrt{\pi}$ are used. In solving Eq. (57) there may be more than one value

of γ satisfying the equation, the lowest value which satisfies the condition

$\gamma \geqslant m$ is taken. Then this value is substituted in the field equations (56)

to get the lowest mode in the horn, which corresponds to the TE_{10} in the rec-

tangular waveguide.

2.5.1 <u>Radiation</u> <u>Field</u> <u>of</u> <u>the</u> <u>Horn</u>.[6,8]—The field at the point P is given

by

$$\bar{E}_p = -\frac{jk_1}{4\pi R} e^{-jk_1 R}\bar{R}_1 \times \int_A \left[\bar{n} \times \bar{E} - \left(\frac{\mu_1}{\epsilon_1}\right)^{\frac{1}{2}} \bar{R}_1 \times (\bar{n} \times \bar{H})\right] e^{jk_1\bar{\rho}_0\bar{R}_1}ds \quad (59)$$

The origin is the center of the sphere of which the horn is a part; r_2, θ, ϕ

define a point on the aperture; R, θ', ϕ' define the field point; $\bar{R}_1$ is a unit

vector in direction of R; $\bar{\rho}$ is the vector from the origin to the element ds on

the surface of the aperture; $\bar{n}$ is the outward normal to the aperture.

$$\bar{n} \times \bar{E} = \bar{a}_r \times [E_\theta\bar{a}_\theta + E_\phi\bar{a}_\phi] = E_\theta\bar{a}_\phi - E_\phi\bar{a}_\theta$$

$$\bar{n} \times \bar{H} = \bar{a}_r \times [H_r\bar{a}_r + H_\theta\bar{a}_\theta + H_\phi\bar{a}_\phi] = H_\theta\bar{a}_\phi - H_\phi\bar{a}_\theta$$

$$\bar{\rho} = r_2\sin\theta\cos\phi\bar{a}_r + r_2\sin\theta\sin\phi\bar{a}_y + r_2\cos\theta\bar{a}_z$$

$$\bar{R}_1 = \sin\theta'\cos\phi'\bar{a}_x' + \sin\theta'\sin\phi'\bar{a}_y' + \cos\theta'\bar{a}_z' \quad (60)$$

From Fig. 13 it is seen that

$$\bar{a}_y' = \bar{a}_z$$

$$\bar{a}_x' = -\sin\frac{\phi_1}{2}\bar{a}_x + \cos\frac{\phi_1}{2}\bar{a}_y \quad (61)$$

$$\bar{a}_z' = \cos\frac{\phi_1}{2}\bar{a}_x + \sin\frac{\phi_1}{2}\bar{a}_y$$

52

Note that the field point is defined with respect to the axes x', y', z'; the axis z' passes by the center of the aperture, while the x axis passes by the the center of the boundary $\phi = 0$, as shown in Fig. 13.

From Eqs. (60) and (61) we get

$$\bar{\rho} \cdot \bar{R}_1 = - r_2 \sin \theta \cos \phi \sin \theta' \cos \phi' \sin \frac{\phi_1}{2} + r_2 \sin \theta \cos \phi \cos \theta' \cos \frac{\phi_1}{2}$$
$$+ r_2 \sin \theta \sin \phi \sin \theta' \cos \phi' \cos \frac{\phi_1}{2} + r_2 \sin \theta \sin \phi \cos \theta' \sin \frac{\phi_1}{2}$$
$$+ r_2 \cos \theta \sin \theta' \sin \phi' \tag{62}$$

For the plane $\phi' = \frac{\pi}{2}$, Eq. (62) reduces to

$$\bar{\rho} \cdot \bar{R}_1 = r_2 \sin \theta \cos \phi \cos \theta' \cos \frac{\phi_1}{2} + r_2 \sin \theta \sin \phi \cos \theta' \sin \frac{\phi_1}{2} + r_2 \cos \theta$$
$$\sin \theta'$$
$$= r_2 [\sin \theta \cos \theta' \cos(\phi - \frac{\phi_1}{2}) + \cos \theta \sin \theta'] \tag{63}$$

Also Eq. (60) reduces to

$$\bar{R}_1 = \sin \theta' \bar{a}_y' + \cos \theta' \bar{a}_z' \tag{64}$$

Therefore Eq. (59) reduces to

$$\bar{E}_p(\theta') = - \frac{jk_1 r_2^2 e^{-jk_1 R}}{4\pi R} \bar{R}_1 \times \int_0^{\phi_1} \int_{\theta_1}^{\pi-\theta_1} \left[(E_\theta \bar{a}_\phi - E_\phi \bar{a}_\theta) - (\frac{\mu_1}{\epsilon_1})^{\frac{1}{2}} \bar{R}_1 \times (H_\theta \bar{a}_\phi - H_\phi \bar{a}_\theta) \right] e^{jk_1 r_2 [\sin \theta \cos \theta' \cos(\phi - \frac{\phi_1}{2}) + \cos \theta \sin \theta']} \sin \theta d\theta d\phi \tag{65}$$

Now let us put the integrand in terms of x', y' and z' components.

Referring to Fig. 13,

$$\bar{a}_\phi = - \sin \phi \bar{a}_x + \cos \phi \bar{a}_y$$
$$\bar{a}_\theta = - \sin \theta \bar{a}_z + \cos \theta \cos \phi \bar{a}_x + \cos \theta \sin \phi \bar{a}_y \tag{66}$$
$$\bar{a}_r = \cos \theta \bar{a}_z + \sin \theta \cos \phi \bar{a}_x + \sin \theta \sin \phi \bar{a}_y$$

$$\overline{R}_1 \times (E_\theta \overline{a}_\phi - E_\phi \overline{a}_\theta)$$

$$= (\sin \theta' \overline{a}_y' + \cos \theta' \overline{a}_z') \times [E_\theta(- \sin \phi \overline{a}_x + \cos \phi \overline{a}_y)$$

$$- E_\phi(- \sin \theta \overline{a}_z + \cos \theta \cos \phi \overline{a}_x + \cos \theta \sin \phi \overline{a}_y)] \qquad (67)$$

and let us express $\overline{a}_x$, $\overline{a}_y$, $\overline{a}_z$ in terms of $\overline{a}_x'$, $\overline{a}_y'$, $\overline{a}_z'$:

$$\overline{a}_z = \overline{a}_y'$$

$$\overline{a}_x = - \sin \frac{\phi_1}{2} \overline{a}_x' + \cos \frac{\phi_1}{2} \overline{a}_z' \qquad (68)$$

$$\overline{a}_y = \cos \frac{\phi_2}{2} \overline{a}_x' + \sin \frac{\phi_2}{2} \overline{a}_z'$$

Substituting from Eq. (68) in Eq. (67),

Therefore

$$\overline{R}_1 \times (E_\theta \overline{a}_\phi - E_\phi \overline{a}_\theta)$$

$$= (\sin \theta' \overline{a}_y' + \cos \theta' \overline{a}_z') \times \left[E_\theta(\sin \phi \sin \frac{\phi_1}{2} \overline{a}_x' - \sin \phi \cos \frac{\phi_2}{2} \overline{a}_z' \right.$$

$$+ \cos \phi \cos \frac{\phi_1}{2} \overline{a}_x' + \cos \phi \sin \frac{\phi_1}{2} \overline{a}_z') - \sin \theta \overline{a}_y' - \cos \theta \cos \phi \sin \frac{\phi_2}{2}$$

$$\overline{a}_x' + \cos \theta \cos \phi \cos \frac{\phi_2}{2} \overline{a}_z' + \cos \theta \sin \phi \cos \frac{\phi_2}{2} \overline{a}_x' + \cos \theta \sin \phi \sin$$

$$\left. \frac{\phi_2}{2} \overline{a}_z') \right]$$

$$= A\overline{a}_x' + B\overline{a}_y' + C\overline{a}_z' \qquad (69)$$

where:

$$A = \sin \theta' \left[E_\theta \sin(\frac{\phi_1}{2} - \phi) - E_\phi \cos \theta \cos(\frac{\phi_1}{2} - \phi) \right]$$

$$- E_\phi \cos \theta' \sin \theta$$

$$B = \cos \theta' \left[E_\theta \cos(\frac{\phi_1}{2} - \phi) + E_\phi \cos \theta \sin(\frac{\phi_1}{2} - \phi) \right] \qquad (70)$$

$$C = - \sin \theta' \left[E_\theta \cos(\frac{\phi_2}{2} - \phi) + E_\phi \cos \theta \sin(\frac{\phi_2}{2} - \phi) \right]$$

$$\overline{R}_1 \times [\overline{R}_1 \times (H_\theta \overline{a}_\phi - H_\phi \overline{a}_\theta)]$$

$$= (\sin \theta' \overline{a}_y' + \cos \theta' \overline{a}_z') \times (A' \overline{a}_x' + B' \overline{a}_y' + C' \overline{a}_z')$$

where A', B', and C' are obtained from A, B, and C, respectively, by putting H instead of E.

Therefore

$$\overline{R}_1 \times [\overline{R}_1 \times (H_\theta \overline{a}_\phi - H_\phi \overline{a}_\theta)]$$

$$= \overline{a}_x'(\sin \theta' C' - \cos \theta' B')$$

$$+ \overline{a}_y' \cos \theta' A'$$

$$+ \overline{a}_z'(-\sin \theta' A') \tag{71}$$

Substituting from Eqs. (70) and (71) into Eq. (65), we get for the plane $\phi' = \pi/2$

$$E_x'(\theta') = - \frac{jk_1 r_2^2}{4\pi R} e^{-jk_1 R} \int_0^{\phi_1} \int_{\theta_1}^{\pi-\theta_1} \Bigg\{ \sin \theta' [E_\theta \sin(\frac{\phi_1}{2} - \phi)$$

$$- E_\phi \cos \theta \cos(\frac{\phi_1}{2} - \phi)] - \cos \theta' \sin \theta E_\phi + (\frac{\mu_1}{\epsilon_1})^{\frac{1}{2}} [H_\theta \cos(\frac{\phi_1}{2} - \phi)$$

$$+ H_\phi \cos \theta \sin(\frac{\phi_1}{2} - \phi)] \Bigg\} \times \exp\Bigg\{ jk_1 r_2 [\sin \theta \cos \theta' \cos(\frac{\phi_1}{2} - \phi)$$

$$+ \cos \theta \sin \theta'] \sin \Bigg\} \theta d\theta d\phi \tag{72}$$

$$E_y'(\theta') = - \frac{jk_1 r_2^2}{4\pi R} e^{-jk_1 R} \int_0^{\phi_1} \int_{\theta_1}^{\pi-\theta_1} \Bigg\{ \cos \theta' [E_\theta \cos(\frac{\phi_1}{2} - \phi)$$

$$+ E_\phi \sin(\frac{\phi_1}{2} - \phi) \cos \theta] - (\frac{\mu_1}{\epsilon_1})^{\frac{1}{2}} \sin \theta' \cos \theta' [H_\theta \sin(\frac{\phi_1}{2} - \phi)$$

$$- H_\phi \cos \theta \cos(\frac{\phi_1}{2} - \phi)] + (\frac{\mu_1}{\epsilon_1})^{\frac{1}{2}} \cos^2\theta' \sin \theta H_\phi \Bigg\}$$

$$\exp\Bigg\{ jk_1 r_2 [\sin \theta \cos \theta' \cos(\phi - \frac{\phi_2}{2}) + \cos \theta \sin \theta] \Bigg\} \times \sin \theta d\theta d\phi \tag{73}$$

$$E_z'(\theta') = -\frac{jk_1 r_2^2}{4\pi R} e^{-jk_1 R} \int_0^{\phi_1} \int_{\theta_1}^{\pi-\theta_1} \left\{ -\sin\theta' [E_\theta \cos(\frac{\phi_1}{2} - \phi) \right.$$

$$+ E_\phi \cos\theta \sin(\frac{\phi_1}{2} - \phi) + (\frac{\mu_1}{\epsilon_1})^{\frac{1}{2}} \sin^2\theta' [H_\theta \sin(\frac{\phi_1}{2} - \phi)$$

$$- H_\phi \cos\theta \cos(\frac{\phi_1}{2} - \phi)] - (\frac{\mu_1}{\epsilon_1})^{\frac{1}{2}} \sin\theta' \cos\theta' \sin\theta E_\phi \Big\}$$

$$\cdot \exp\left\{jk_1 r_2[\sin\theta\cos\theta'\cos(\phi - \frac{\phi_1}{2}) + \cos\theta\sin\theta']\right\}\sin\theta d\theta d\phi \tag{74}$$

Equations (72), (73), and (74) give the radiation field as a function of θ' in terms of the field at the aperture E_θ and E_ϕ which are obtained from Eq. (56) by putting $r = r_2$.

For the plane $\phi' = 0$ substitute in Eq. (62).

Therefore

$$\bar{\rho} \cdot \bar{R}_1 = -r_2 \sin\theta \cos\phi \sin\theta' \sin\frac{\phi_1}{2} + r_2 \sin\theta \cos\phi \cos\theta' \cos\frac{\phi_1}{2}$$

$$+ r_2 \sin\theta \sin\phi \sin\theta' \cos\frac{\phi_1}{2} + r_2 \sin\theta \sin\phi \cos\theta' \sin\frac{\phi_1}{2}$$

$$= r_2 \sin\theta \cos(\phi - \frac{\phi_1}{2} - \theta') \tag{75}$$

$$\bar{R}_1 = \sin\theta \bar{a}_x' + \cos\theta' \bar{a}_z' \tag{76}$$

Therefore

$$\bar{E}_p(\theta') = -\frac{jk_1 r_2^2 e^{-jk_1 R}}{4\pi r} \bar{R}_1 \int_0^{\phi_1} \int_{\theta_1}^{\pi-\theta_1} [E_\theta \bar{a}_\phi - E_\phi \bar{a}_\theta) - (\frac{\mu_1}{\epsilon_1})^{\frac{1}{2}} \bar{R}_1$$

$$\times (H_\theta \bar{a}_\phi - H_\phi \bar{a}_\theta)] \times \exp\left\{jk_1 r_2 \sin\theta \cos(\phi - \frac{\phi_1}{2} - \theta')\right\} \sin\theta d\theta d\phi \tag{77}$$

$$\bar{R}_1 \times (E_\theta \bar{a}_\phi - E_\phi \bar{a}_\theta) = (\sin\theta' \bar{a}_x' + \cos\theta' \bar{a}_z') \times [E_\theta(-\sin\phi \bar{a}_x + \cos\phi \bar{a}_y)$$

$$- E_\phi(-\sin\theta \bar{a}_z + \cos\theta \cos\phi \bar{a}_x + \cos\theta \sin\phi \bar{a}_y)] \tag{78}$$

as before

$$\bar{a}_x = -\sin\frac{\phi_1}{2}\,\bar{a}_x' + \cos\frac{\phi_1}{2}\,\bar{a}_z'$$

$$\bar{a}_y = \cos\frac{\phi_1}{2}\,\bar{a}_x' + \sin\frac{\phi_1}{2}\,\bar{a}_z'$$

$$\bar{a}_z = \bar{a}_y' \tag{79}$$

Therefore

$$\bar{R}_1 \times (E_\theta\bar{a}_\phi - E_\phi\bar{a}_\theta)$$

$$= (\sin\theta'\bar{a}_x' + \cos\theta'\bar{a}_z') \times [-\sin\phi E_\theta(-\sin\frac{\phi_1}{2}\,\bar{a}_x' + \cos\frac{\phi_1}{2}\,\bar{a}_z')$$

$$+ \cos\phi E_\theta(\cos\frac{\phi_1}{2}\,\bar{a}_x' + \sin\frac{\phi_1}{2}\,\bar{a}_z') + \sin\theta E_\phi\bar{a}_y' - \cos\theta\cos\phi E_\phi$$

$$(-\sin\frac{\phi_1}{2}\,\bar{a}_x' + \cos\frac{\phi_1}{2}\,\bar{a}_z') - \cos\theta\sin\phi E_\phi(\cos\frac{\phi_1}{2}\,\bar{a}_x' + \sin\frac{\phi_1}{2}\,\bar{a}_z')]$$

$$= \bar{a}_x'(-\cos\theta'\sin\theta E_\phi) + \bar{a}_y'[E_\theta\cos(\theta' - \phi - \frac{\phi_1}{2})$$

$$+ E_\phi\cos\theta\sin(\theta' - \phi + \frac{\phi_1}{2})] + \bar{a}_z'\sin\theta'\sin\theta E_\phi \tag{80}$$

$$\bar{R}_1 \times [R_1 \times (H_\theta\bar{a}_\phi - H_\phi\bar{a}_\theta)]$$

$$= (\sin\theta'\bar{a}_x' + \cos\theta'\bar{a}_z') \times (F\bar{a}_x' + G\bar{a}_y' + H\bar{a}_z')$$

where F, G, H are the coefficients of $\bar{a}_x'$, $\bar{a}_y'$, $\bar{a}_z'$, respectively, in Eq. (80)

but E is replaced by H.

Therefore

$$\bar{R}_1 \times [\bar{R}_1 \times (H_\theta\bar{a}_\phi - H_\phi\bar{a}_\theta)]$$

$$= -\bar{a}_x'[H_\theta\cos\theta'\cos(\theta' - \phi + \frac{\phi_1}{2}) + H_\phi\cos\theta'\cos\theta\sin(\theta' - \phi + \frac{\phi_1}{2})]$$

$$-\bar{a}_y'(\sin\theta H_\phi)$$

$$+ \bar{a}_z'[H_\theta\sin\theta'\cos(\theta' - \phi - \frac{\phi_1}{2}) + H_\phi\sin\theta'\cos\theta\sin(\theta' - \phi + \frac{\phi_1}{2})]$$

Substituting in Eq. (77), we get for the plane $\phi' = 0$

Therefore

$$E'_x(\Theta') = -\frac{jk_1 r_2^2 e^{-jk_1 R}}{4\pi R} \int_0^{\phi_1} \int_{\Theta_1}^{\pi-\Theta_1} \left\{ -\cos\Theta' \sin\Theta E_\phi + \left(\frac{\mu_1}{\epsilon_1}\right)^{\frac{1}{2}} \right.$$

$$\left[H_\Theta \cos\Theta' \cos\left(\Theta' - \phi - \frac{\phi_1}{2}\right) + H_\phi \cos\Theta' \cos\Theta \sin\left(\Theta' - \phi + \frac{\phi_1}{2}\right) \right]$$

$$\exp\left[jk_1 r_2 x \sin\Theta \cos\left(\Theta' - \phi + \frac{\phi_2}{2}\right) \right] \right\} \sin\Theta \, d\Theta \, d\phi \tag{82}$$

$$E'_y(\Theta') = -\frac{jk_1 r_2^2 e^{-jk_1 R}}{4\pi R} \int_0^{\phi_1} \int_{\Theta_1}^{\pi-\Theta_1} \left[\cos\left(\Theta' - \phi + \frac{\phi_1}{2}\right) E_\Theta \right.$$

$$\left. + \cos\Theta \sin\left(\Theta' - \phi + \frac{\phi_2}{2}\right) E_\phi + \left(\frac{\mu_1}{\epsilon_1}\right)^{\frac{1}{2}} \sin\Theta H_\phi \right]$$

$$\exp\left[jk_1 r_2 \sin\Theta \cos\left(\Theta' - \phi + \frac{\phi_1}{2}\right) \right] \sin\Theta \, d\Theta \, d\phi \tag{83}$$

$$E'_z(\Theta') = -\frac{jk_1 r_2^2 e^{-jk_1 R}}{4\pi R} \int_0^{\phi_1} \int_{\Theta_1}^{\pi-\Theta_1} \left\{ \sin\Theta' \sin\Theta E_\phi - \left(\frac{\mu_1}{\epsilon_1}\right)^{\frac{1}{2}} \right.$$

$$\left[H_\Theta \sin\Theta' \cos\left(\Theta' - \phi + \frac{\phi_1}{2}\right) + H_\phi \sin\Theta' \cos\Theta \sin\left(\Theta' - \phi + \frac{\phi_1}{2}\right) \right]$$

$$\exp jk_1 r_2 \sin\Theta \cos\left(\Theta' - \phi + \frac{\phi_1}{2}\right) \right\} x \sin\Theta \, d\Theta \, d\phi \tag{84}$$

Equations (82), (83), and (84) give the radiation field in terms of the fields E_Θ and E_ϕ at the aperture.

The integrations occurring in the radiation field expressions are of the form:

$$\int_0^{\phi_1} \sin\frac{\pi\phi}{\phi_1} \sin\left(\frac{\phi_1}{2} - \phi\right) e^{jb \cos\left(\phi - \frac{\phi_1}{2}\right)} d\phi$$

The integrand is a trigonomentric function multiplied by an exponential function. The integrals can be evaluated by computer methods.

3. ACTIVITIES FOR THE NEXT PERIOD

Computer facilities will not be available until October 15 while the IBM-704 is being replaced by an IBM-709 computer. Computer programs presently in use can be used directly on the nex computer. As soon as the new computer is in operation, the computer results will be obtained on the details of power flow near resonance in the studies of sphere and cylinder diffraction. In addition, computer results will be obtained on the diffraction by a magnetized ferrite cylinder.

Experimental work is presently being conducted on a biconical antenna, a ferrite-filled cavity backed slot antenna, a ferrite-filled disk antenna, a shielded ferrite-loaded balanced loop antenna, and a coaxial fed ferrite-loaded disk antenna. In addition, a ridged ferrite-loaded cavity-backed slot antenna is being constructed. Work on approximately half of these antennas in nearing completion and will be summarized in the next quarterly report.

The computer results on the sectoral horn analysis are being studied at present and will be given in the next quarterly report.

During the next period several new theoretical studies will be initiated, including a variational solution of the radiation from a ferrite-loaded cavity backed slot antenna; a study of the radiation from a constant current antenna surrounded by a ferrite prolate spheroid; and studies of antennas immersed in ion plasmas.

4. SUMMARY

The theoretical study of plane wave diffraction by a ferrite sphere has been extended to treat a lossy sphere enclosed within the ferrite sphere. Computer results show that the power absorbed by the lossy sphere rises to values greater than 500 times the power incident upon a cross-sectional area in free space equal to that of the large ferrite sphere.

Computer results have been obtained for the total power flow through a long ferrite cylinder with an incident plane wave. The total power exhibits resonances where the total power rises to values greater than ten times the power that would pass through a cross-sectional area in free space equal to that of the cylinder.

A study of plane wave diffraction by a ferrite prolate spheroid has been initiated and the preliminary analytical steps have been carried out. Because of the urgencies of other parts of the project effort, the study has been discontinued and will not be started again unless developments in other areas indicate that the results would be significant. The radiation from a material-filled rectangular waveguide sectoral horn has been analyzed and computer results are being obtained. The radiation from a ferrite-filled double taper horn fed by a rectangular waveguide has been analyzed mathematically. This problem is also quite complex and, unless further developments indicate a significance, probably will not be evaluated on the computer. Results are already being obtained on the single taper sectoral horn. The

efforts of project members are now being directed to practical antennas utilizing ferrite materials and which are capable of relatively precise experimental evaluation.

The bibliography has been omitted from this quarterly report in the interest of conserving space. A new bibliography will be compiled and published towards the end of the present contract.

REFERENCES

1. J. A. Stratton, _Electromagnetic Theory_, New York, McGraw-Hill Book Co., Inc., 1941.

2. F. V. Schultz, "Scattering by a Prolate Spheroid," Aeronautical Research Center, The University of Michigan, External Memorandum, No. UMM-42.

3. J. A. Stratton, P. M. Morse, L. J. Chu, and R. A. Hutner, _Elliptic Cylinder and Spheroidal Wave Functions_, John Wiley and Sons, New York, 1941.

4. Carson Flammer, _Spheroidal Wave Functions_, Stanford University Press, Stanford, California, 1957.

5. "The Theory of Electromagnetic Waves," A symposium sponsored by NYU and AFCRC, Interscience Publishers Inc., New York, 1951.

6. S. Silver, "Microwave Antenna Theory and Design," Rad. Lab. Series, Vol. 12, McGraw-Hill, New York, 1949.

7. S. Schelkunoff, _Applied Mathematics for Engineers and Scientists_, D. Van Nostrand Publishing Co.

8. L. J. Chu, "Calculation of Radiation Properties of Hollow Pipes and Horns," _Journal of Applied Physics_, pp. 603-610, September, 1940.